ISSN 2348-375X

Unique Journal of Engineering and Advanced Sciences

Available online: www.ujconline.net

Research Article

COMPETITION KINETICS OF RADICAL-CHAIN ADDITION TO DOUBLE MOLECULAR BONDS

Michael M. Silaev*

Department of Chemistry, Lomonosov Moscow State University, Vorobievy Gory, Moscow 119991, Russia

Received: 14-06-2014; Revised: 12-07-2014; Accepted: 10-08-2014

*Corresponding Author: Michael M. Silaev

Department of Chemistry, Lomonosov Moscow State University, Vorobievy Gory, Moscow 119991, Russia

ABSTRACT

Five reaction schemes are suggested for the initiated nonbranched-chain addition of free radicals to the multiple bonds of the unsaturated compounds. The proposed schemes include the reaction competing with chain propagation reactions through a reactive free radical. The chain evolution stage in these schemes involves three or four types of free radicals. One of them is relatively low-reactive and inhibits the chain process by shortening of the kinetic chain length. Based on the suggested schemes, nine rate equations (containing one to three parameters to be determined directly) are deduced using quasi-steady-state treatment. These equations provide good fits for the nonmonotonic (peaking) dependences of the formation rates of the molecular products (1:1 adducts) on the concentration of the unsaturated component in binary systems consisting of a saturated component (hydrocarbon, alcohol, etc.) and an unsaturated component (olefin, allyl alcohol, formaldehyde, or dioxygen). The unsaturated compound in these systems is both a reactant and an autoinhibitor generating low-reactive free radicals. A similar kinetic description is applicable to the nonbranched-chain process of the free-radical hydrogen oxidation, in which the oxygen with the increase of its concentration begins to act as an oxidation autoinhibitor (or an antioxidant). The energetics of the key radical-molecule reactions is considered.

Keywords: Binary System, Unsaturated Compound, Low-Reactive Radical, Autoinhibitor, Competing Reaction, Non-Branched-Chain Addition, Kinetic Equation, Rate, Parameters, Thermochemical Data, Energy

INTRODUCTION

In a binary system consisting of a saturated component and an unsaturated one, the abstraction of the most labile atom from a saturated molecule by some initiator converts this molecule into a saturated free radical (addend) capable of adding to the double bond of an unsaturated molecule to yield a saturated 1:1 adduct radical. At a sufficiently high concentration of the unsaturated component in the system, this primary adduct radical can add to another unsaturated molecule under certain conditions to yield a secondary, 1:2 adduct radical, and so on, resulting in telomerization. Under other conditions and at other relative reactivities of the components, the concentration of the saturated component can exceed the concentration of the unsaturated component so greatly that the most likely reaction for the primary adduct radical will be the abstraction of the least strongly bonded atom from a saturated molecule rather than addition. This reaction will yield a 1:1 adduct molecule as the ultimate product (it proceeds via a non-branched-chain mechanism since it regenerates the saturated free radical carrying the chain). This reaction may compete with the parallel reaction between the 1:1 adduct radical and an unsaturated molecule. Even at a low concentration of the unsaturated component, this parallel reaction can proceed more efficiently owing to the formation, from the unsaturated molecule, of a free radical stabilized by the delocalization of the unpaired *p*-electron over, e.g., a system of conjugate bonds. This comparatively nonreactive radical does not participate in further chain propagation and inhibits the chain process, being consumed through reactions with the same radical and with the saturated addend radical. If the adduct radical abstracts some labile atom from an unsaturated molecule, it will again turn into the 1:1 adduct molecule, this time via a non-chain mechanism. The 1:1 adduct radical (which is the heaviest and the largest among the free radicals that result from the addition of one addend radical to the double bond of the molecule) may have an increased energy owing to the energy liberated in the transformation of a C=O, C=C, or O=O double bond into an ordinary bond (30–130 kJ mol^{-1} for the gas phase under standard conditions[1–4]). Therefore, it can decompose or react with one of the surrounding molecules in the place of its formation without

diffusing in the solution and, hence, without participating in radical-radical chain termination reactions. Which of the two reactions of the adduct radical, the reaction with the saturated component or the reaction with the unsaturated component, dominates the kinetics of the process will depend on the reactivity and concentration ratios of the components in the binary system. In the processes of this kind, in which an addend radical and a low-reactivity, inhibiting radical are involved in three types of quadratic-law chain termination reactions, the formation rate of the 1:1 adduct as a function of the concentration of the unsaturated component has a maximum (which usually occurs at a low concentration of this component).

Earlier[5,6], there were attempts to describe such peaking dependences fragmentarily, assuming that the saturated or unsaturated component is in excess, in terms of the direct and inverse proportionalities, respectively, that result from the simplification of a particular case of the kinetic equation set up by the quasi-steady-state treatment of binary copolymerization involving fairly long chains[5]. This specific equation is based on an irrational function, whose plot is a monotonic curve representing the dependence of the product formation rate on the concentration of the unsaturated component. This curve comes out of the origin of coordinates, is convex upward, and has an asymptote parallel to the abscissa axis. Replacing the component concentrations with the corresponding mole fractions generates a peak in this irrational function and thereby makes it suitable to describe the experimental data[7]. However, this circumstance cannot serve as a sufficient validation criterion for the mechanism examined, because the new property imparted to the function by the above artificial transformation does not follow from the solution of the set of algebraic equations that are set up for the reaction scheme accepted for the process in a closed system and express the equality of the steady-state formation and disappearance rates of the reactive intermediates.

This publication presents a comprehensive review of the non-branched-chain kinetic models developed for particular types of additions of saturated free radicals to multiple bonds[8-14]. It covers free radical additions to alkenes[10,11], their derivatives[8,9], formaldehyde (first compound in the aldehyde homological series)[8,9,12], and oxygen[13,14] (which can add an unsaturated radical as well) yielding various 1:1 molecular adducts, whose formation rates as a function of the unsaturated compound concentration pass through a maximum (free radical chain additions to the C=N bond have not been studied adequately). In the kinetic description of these non-telomerization chain processes, the reaction between the 1:1 adduct radical and the unsaturated molecule, which is in competition with chain propagation through a reactive free radical ($^{\bullet}PCl_2$, $C_2H_5\dot{C}HOH$, etc.), is included for the first time in the chain propagation stage. This reaction yields a low-reactive radical (such as $CH_2=C(CH_3)\dot{C}H_2$ or $H\dot{C}=O$) and thus leads to chain termination because this radical does not continue the chain and thereby inhibits the chain process[8]. We will consider kinetic variants for the case of comparable component concentrations with an excess of the saturated component[10,11] and the case of an overwhelming excess of the saturated component over the unsaturated component[8,9,12].

Based on the reaction schemes suggested for the kinetic description of the addition process, we have derived kinetic equations with one to three parameters to be determined directly. Reducing the number of unknown parameters in a kinetic equation will allow one to decrease the narrowness of the correlation of these parameters and to avoid a sharp build-up of the statistical error in the nonlinear estimation of these parameters in the case of a limited number of experimental data points[15]. The rate constant of the addition of a free radical to the double bond of the unsaturated molecule, estimated as a kinetic parameter, can be compared to its reference value if the latter is known. This provides a clear criterion to validate the mathematical description against experimental data. The kinetic equations were set up using the quasi-steady-state treatment. This method is the most suitable for processes that include eight to ten or more reactions and four to six different free radicals and are described by curves based on no more than three to seven experimental points. In order to reduce the exponent of the $2k_5[R_1^{\bullet}]^2$ term in the $d[R_1^{\bullet}]/dt = 0$ equation to unity[8], we used the following condition for the early stages of the process: $k_6 = \sqrt{2k_5 2k_7}$ [16] and, hence, $V_1 = V_5 + 2V_6 + V_7 = (\sqrt{2k_5}\,[R_1^{\bullet}] + \sqrt{2k_7}\,[R_2^{\bullet}])^2$. Here, $[R_1^{\bullet}]$ and $[R_2^{\bullet}]$ are the concentrations of the addend radical and the low-reactive (inhibitor) radical, respectively; V_1 is the initiation rate; V_5, $2V_6$, and V_7 are the rates of the three types of diffusion-controlled quadratic-law chain termination reactions; $2k_5$ and $2k_7$ are the rate constants of the loss of identical free radicals via the reactions $R_1^{\bullet} + R_1^{\bullet}$ and $R_2^{\bullet} + R_2^{\bullet}$, respectively; k_6 is the rate constant of the loss of different free radicals via the $R_1^{\bullet} + R_2^{\bullet}$ reaction (see *Schemes* 1–5). The kinetic equations thus obtained fit the peaking rate curves well throughout the range of unsaturated component concentrations in the binary systems. Our mathematical simulation was based on experimental data obtained for γ-radiation-induced addition reactions for which the initiation rate V_1 is known. The analysis of stable liquid-phase products was carried out by the gas chromatographic method.

RESULTS AND DISCUSSION

1. Addition to the C=C Bond of Alkenes and Their Derivatives

When reacting with alkenes not inclined to free-radical polymerization, the free radicals originating from inefficient saturated telogens, such as alcohols[17] and amines[18], usually add to the least substituted carbon atom at the double bond, primarily yielding a free 1:1 adduct radical. This radical accumulates an energy of 90–130 kJ mol^{-1}, which is released upon the transformation of the C=C bond to an ordinary bond (according to the data reported for the addition of nonbranched C_1–C_4 alkyl radicals to propene and of similar C_1 and C_2 radicals to 1-butene in the gas phase under standard conditions[1-4]. Such adduct radicals, which do not decompose readily for structural reasons, can abstract the most labile atom from a neighbour molecule of the saturated or unsaturated component of the binary reaction system, thus turning into a 1:1 adduct molecule. The consecutive and parallel reactions

involved in this free-radical nonbranched-chain addition process are presented below (*Scheme 1*). In the case of comparable component concentrations with a nonoverwhelming excess of the saturated component, extra reaction (1b) ($k_{1b} \neq 0$) is included in the initiation stage[10,11]. In the case of an overwhelming excess of the saturated component reaction (1b) is ignored ($k_{1b} = 0$)[8,9,12].

1.1 Comparable Component Concentrations

Scheme 1

Chain initiation

1. $I \xrightarrow{2k_1} 2R_0^{\bullet}$;

1a. $R_0^{\bullet} + R_1A \xrightarrow{k_{1a}} R_0A + R_1^{\bullet}$;

1b. $R_0^{\bullet} + R_2A \xrightarrow{k_{1b}} R_0A + R_2^{\bullet}$.

Chain propagation

2. $R_1^{\bullet} + R_2B \xrightarrow{k_2} R_3^{\bullet}$;

3. $R_3^{\bullet} + R_1A \xrightarrow{k_3} R_3A + R_1^{\bullet}$.

Inhibition

4. $R_3^{\bullet} + R_2B \xrightarrow{k_4} R_3B + R_2^{\bullet}$.

Chain termination

5. $2R_1^{\bullet} \xrightarrow{2k_5}$ Prod;

6. $R_1^{\bullet} + R_2^{\bullet} \xrightarrow{k_6}$ Prod;

7. $2R_2^{\bullet} \xrightarrow{2k_7}$ Prod.

In this scheme, I is an initiator (e.g., a peroxide[5,12,13]); $R_0^{\bullet}$ is a reactive (initiating) radical; A and B are hydrogen or halogen atoms[2,5,17-24]; $R_1^{\bullet}$ is $^{\bullet}PCl_2$[19], $^{\bullet}CCl_3$[20], alkyl[2,5], 1-hydroxyalkyl[5,6,17,22-24], or a similar functionalized reactive addend radical[5]; $R_2^{\bullet}$ is an alkenyl radical (allyl or higher)[2,5,17,22], 1-hydroxyalkenyl[5,17,18,23,24], or a similar functionalized low-reactive (inhibitor) radical[5,18]; $R_3^{\bullet}$ is a saturated reactive 1:1 adduct radical; R_0A, R_0B, and R_1A are saturated molecules; R_2B is an unsaturated molecule (olefin or its derivative); R_3A and R_3B are 1:1 adduct molecules; Prod designates the molecular products resulting from the dimerization or disproportionation of free radicals. The chain evolution (propagation and inhibition) stage of *Scheme 1* include consecutive reactions 2 and 3, parallel (competing) reaction pairs 3 and 4, and consecutive-parallel reaction pair 2–4.

The initiation reaction 1 is either the decomposition of a chemical initiator[5,17,18] or a reaction induced by light [5,17,18] or ionizing radiation[19-23]. The overall rate of chain initiation (reactions 1, 1a, and 1b) is determined by the rate of the rate-limiting step ($k_{1b} > k_{1a}$). The reaction between the free radical $R_2^{\bullet}$, which results from reactions 1b and 4, and the saturated molecule R_1A is energetically unfavorable because it implies the formation of the free radical $R_1^{\bullet}$, which is less stable than the initial one. The addition reaction 2 may be accompanied by the abstraction reaction 2a. $R_1^{\bullet} + R_2B \xrightarrow{k_{2a}} R_1B + R_2^{\bullet}$ which yields the product R_1B *via* a nonchain mechanism. Reaction 2a does not regenerate the addend radical $R_1^{\bullet}$ and is not necessary for a kinetic description of the process, because the rate ratio of reactions 2 and 2a, $V_2/V_{2a} = k_2/k_{2a}$, is independent of the concentration of the unsaturated component R_2B in the system. The inhibition of the nonbranched-chain addition process is due to reaction 4, in which the adduct radical $R_3^{\bullet}$ is spent in an inefficient way, since this reaction, unlike reaction 3, does not regenerate $R_1^{\bullet}$. The inhibiting effect is also due to the loss of chain carriers $R_1^{\bullet}$ through their collisions with low-reactive unsaturated radicals $R_2^{\bullet}$, but to a much lesser extent.

The rates of the formation (V, mol dm^{-3} s^{-1}) of the 1:1 adducts R_3A (*via* a chain mechanism) and R_3B (*via* a nonchain mechanism) in reactions 3 and 4 are given by the equations

$$V_3(R_3A) = \frac{[\gamma l/(\gamma l + x)]V_1 \alpha l k_2 x}{k_2 x^2 + (\alpha l + x)\sqrt{2k_5 V_1}}, \quad (1)$$

$$V_4(R_3B) = \frac{[\gamma l/(\gamma l + x)]V_1 k_2 x^2}{k_2 x^2 + (\alpha l + x)\sqrt{2k_5 V_1}}, \quad (2)$$

where V_1 is the rate of the initiation reaction 1; $l = [R_1A]$ and $x = [R_2B]$ are the molar concentrations of the initial components, with $l > x$; k_2 is the rate constant of the addition of the $R_1^{\bullet}$ radical from the saturated component R_1A to the unsaturated molecule R_2B (reaction 2); and $\gamma = k_{1a}/k_{1b}$ and $\alpha = k_3/k_4$ are the rate constant ratios for competing (parallel) reactions (α is the first chain-transfer constant for the free-radical telomerization process[5]). The rate ratio for the competing reactions is $V_3/V_4 = \alpha l/x$, and the chain length is $\nu = V_3/V_1$.

Earlier mathematical simulation[8] demonstrated that replacing the adduct radical R_3 with the radical R_2[5] in the reaction between identical radicals and in the reaction involving R_1 gives rise to a peak in the curve of the 1:1 adduct formation rate as a function of the concentration of the unsaturated component. Reaction 1b, which is in competition with reaction 1a, is responsible for the maximum in the curve described by Eq. (2), and reaction 4, which is in competition with reaction (3), is responsible for the maximum in the curve defined by Eq. (1).

The number of unknown kinetic parameters to be determined directly (k_2, α, and γ) can be reduced by introducing the condition $\gamma \cong \alpha$, which is suggested by the chemical analogy between the competing reactions pairs 1a–1b and 3–4. For example, the ratios of the rate constants of the reactions of $^{\bullet}OH$, $CH_3O^{\bullet}$, $^{\bullet}CH_3$, $NO_3^{\bullet}$, and $H_2PO_4^{\bullet}$ with methanol to the rate constants of the reactions of the same radicals with ethanol in aqueous solution at room temperature are 0.4–0.5 [25,26]. For the same purpose, the rate constant of reaction 2 in the kinetic equation can be replaced with its analytical

expression $k_2 = \alpha l_m \sqrt{2k_5V_1} \Big/ x_m^2$, which is obtained by solving the quadratic equation following from the reaction rate extremum condition $\partial V_{3,4}(1:1\,\text{Adduct})/\partial x = 0$, where $\partial V_{3,4}(1:1\,\text{Adduct}) = V_3 + V_4$. After these transformations, the overall formation rate equation for the 1:1 adducts R_3A and R_3B (which may be identical, as in the case of R_3H [5,8,9,12,13,18–21]), appears as

$$V_{3,4}(1{:}1\ \text{Adduct}) = \frac{V_1\alpha l k_2 x}{k_2x^2 + (\alpha l + x)\sqrt{2k_5V_1}} = \quad (3)$$

$$= \frac{V_1\alpha l x}{x^2 + (\alpha l + x)x_m^2 \Big/ \alpha l_m}, \quad (3a)$$

where l_m and x_m are the component concentrations l and x at the points of maximum of the function. Provided that V_1 is known, the only parameter in Eq. (3a) to be determined directly is α. If V_1 is known only for the saturated component R_1A, then, for the binary system containing comparable R_1A and R_2B concentrations, it is better to use the quantity λV_1, where $\lambda = l/(l + x)$ is the mole fraction of R_1A, in place of V_1 in Eqs. (3) and (3a).

The two variable concentrations in the kinetic equation (3) – l and x – can be reduced to one variable by replacing them with the corresponding mole fractions. Substituting the expression $k_2 = \left\{\alpha\left[(1/\chi_m) - 1\right]^2 - 1\right\}\sqrt{2k_5V_1}\Big/(l_m + x_m)$, derived from the rate extremum condition, into this transformed equation for the binary system containing comparable component concentrations, we obtain

$$V_{3,4}(\text{Adduct 1:1}) = \frac{V_1\alpha(1-\chi)\chi}{\chi^2 + [\alpha(1-\chi)+\chi]\Big/\left\{\alpha[(1/\chi_m)-1]^2 - 1\right\}}, \quad (3b)$$

where $1 - \chi = l/(l + x)$ and $\chi = x/(l + x)$ are the mole fractions of the components R_1A and R_2B ($0 < \chi < 1$), respectively, and χ_m is the χ value at the point of maximum.

The overall formation rate of the 1:1 adducts R_3A and R_3B is a sophisticated function of the formation and disappearance rates of the radicals $R_1^\bullet$ and $R_2^\bullet$: $V(R_3A, R_3B) = (V_{1a} + V_3 - V_5) - (V_{1b} + V_4 - V_7)$.

The application of the above rate equations to particular single nonbranched-chain additions is illustrated in Fig. 1. Curve *1* represents the results of simulation in terms of Eq. (3b) for the observed 1:1 adduct formation rate as a function of the mole fraction of the unsaturated component in the phosphorus trichloride–methylpropene[1] reaction system at 303 K[19]. In this simulation, the ^{60}Co γ-radiation dose rate was set at $P = 0.01$ Gy s^{-1} and the initiation yield was taken to be $G(^\bullet PCl_2) = 2.8$ particles per 100 eV (1.60×10^{-17} J) of the energy absorbed by the solution[19]. The product of reaction 3 is $Cl_2PCH_2C(Cl)(CH_3)CH_3$ (two isomers), $V_1 = 4.65 \times 10^{-9}$ mol dm^{-3} s^{-1} at $\chi = 0$, and $2k_5 = 3.2 \times 10^8$ dm^3 mol^{-1} s^{-1}. This leads to $\alpha = (2.5 \pm 0.4)\times 10^3$, and the rate constant of reaction 2 derived from this α value is $k_2 = (1.1 \pm 0.2) \times 10^4$ dm^3 mol^{-1} s^{-1}.

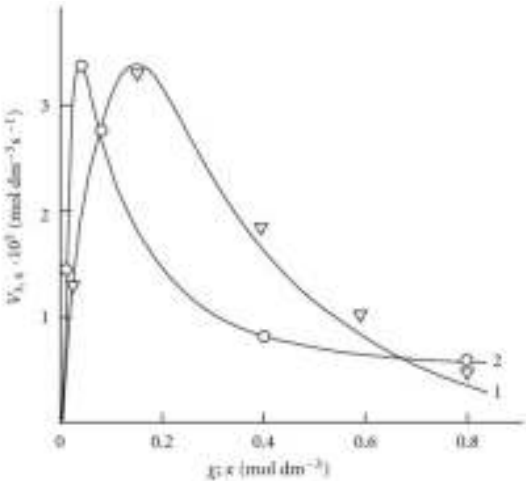

Figure 1: Reconstruction of the functional dependences (curves) of the product formation rates $V_{3,4}$ (*1*, ∇) on the mole fraction of the unsaturated component (χ) from empirical data (symbols) using Eq. (3b) (model optimization with respect to the parameter α) for the phosphorus trichloride–methylpropene reaction system at 303 K [19] (standard deviation of $S_Y = 2.58 \times 10^{-6}$) and (*2*, ○) on the concentration of the unsaturated component (x) from empirical data (symbols) using Eq. (4a) (model optimization with respect to V_1, x_m, and α) for the 2-propanol–2-propen-1-ol system at 433 K [23] ($S_Y = 5.91 \times 10^{-7}$).

Note that, if the R_2–B bond dissociation energy for the unsaturated component of the binary system is approximately equal to or above, not below, the R_1–A bond dissociation energy for the saturated component, than the rate of reaction 4 relative to the rate of the parallel reaction 3 (chain propagation through the reactive free radical $R_1^\bullet$) will be sufficiently high for adequate description of R_3A and R_3B adduct formation in terms of Eqs. (1)–(3b) only at high temperatures[20]. In the phosphorus trichloride–propene system, the difference between the R_2–B (B = H) and R_1–A (A = Hal) bond dissociation energies in the gas phase under standard conditions[1] is as small as 5 kJ mol^{-1}, while in the tetrachloromethane–methylpropene (or cyclohexene) and bromoethane–2-methyl-2-butene systems, this difference is 20.9 (37.7) and ~24 kJ mol^{-1}, respectively.

1.2 Excess of the Saturated Component

If the concentration of the saturated component exceeds the concentration of the unsaturated component in the binary system, reaction 1b can be neglected. If this is the case ($k_{1b} = 0$), then, in the numerators of the rate equations for reactions 3 and 4 (Eqs. (1) and (2)), $\gamma l/(\gamma l + x) = 1$ and the overall rate equation for the formation of the 1:1 adducts R_3A and R_3B will appear as

$$V_{3,4}(1{:}1\ \text{Addduct}) = \frac{V_1(\alpha l + x)k_2 x}{k_2x^2 + (\alpha l + x)\sqrt{2k_5V_1}} = \quad (4)$$

$$= \frac{V_1 x}{\dfrac{x^2}{\alpha l + x} + \left(\dfrac{\sqrt{\alpha l_m}}{x_m} + \dfrac{1}{\sqrt{\alpha l_m}}\right)^{-2}}, \quad (4a)$$

[1] In an earlier work[10], the methylpropene concentration in this system was overvalued by a factor of 1.7 when it was derived from the mole fractions given in[19].

where the parameters are designated in the same way as in Eqs. (1)–(3a), $l >> x$, and

$k_2 = \left[\left(\sqrt{\alpha l_m}/x_m\right) + \left(1/\sqrt{\alpha l_m}\right)\right]^2 \sqrt{2k_5V_1}$ is determined from the condition $\partial V_{3,\,4}(1{:}1\ \text{Adduct}) / \partial x = 0$.

The rate equations for the chain termination reactions 5–7 (*Scheme 1*, $k_{1b} = 0$) are identical to Eqs. (9)–(11) (see below) with $\beta = 0$.

Note that, if it is necessary to supplement *Scheme 1* for $k_{1b} = 0$ with the formation of R_1B *via* the possible nonchain reaction 2a (which is considered in the Section 1.1), the parameter k_{2a} should be included in the denominator of Eq. (4) to obtain

$$k_2x^2 + (\alpha l + x)(k_{2a}x + \sqrt{2k_5V_1}).$$

The analytical expression for k_2 in the case of $k_{2a} \neq 0$ is identical to the expression for k_2 for Eq. (4). The equation for the rate $V_{2a}(R_1B)$ can be derived by replacing k_2 with k_{2a} in the numerator of Eq. (4) containing k_{2a} in its denominator.

Curve *2* in Fig. 1 illustrates the good fit between Eq. (4a) and the observed 1:1 adduct formation rate as a function of the concentration of the unsaturated component in the reaction system 2-propanol–2-propen-1-ol at 433 K[8,9]. In this description, we used a ^{60}Co γ-radiation dose rate of P = 4.47 Gy s^{-1}. The product of reactions 3 and 4 is $CH_3(CH_3)C(OH)CH_2CH_2CH_2OH$, and $2k_5 = 1.0 \times 10^{10}$ dm^3 mol^{-1} s^{-1}. The following parameters were obtained: $V_1 = (3.18 \pm 0.4) \times 10^6$ mol dm^{-3} s^{-1}, $x_m = (3.9 \pm 0.5) \times 10^{-2}$ mol dm^{-3}, and $\alpha = (6.8 \pm 0.8) \times 10^{-2}$. The rate constant of reaction 2 derived from this α is $k_2 = (1.0 \pm 0.14) \times 10^5$ dm^3 mol^{-1} s^{-1}.

2. Addition to the C=O Bond of Formaldehyde

Free radicals add to the carbon atom at the double bond of the carbonyl group of dissolved free (unsolvated, monomer) formaldehyde. The concentration of free formaldehyde in the solution at room temperature is a fraction of a percent of the total formaldehyde concentration, which includes formaldehyde chemically bound to the solvent[27]. The concentration of free formaldehyde exponentially increases with increasing temperature[28]. The energy released as a result of this addition, when the C=O bond is converted into an ordinary bond, is 30 to 60 kJ mol^{-1} (according to the data on the addition of C_1–C_4 alkyl radicals in the gas phase under standard conditions[1-4]. The resulting free 1:1 adduct radicals can both abstract hydrogen atoms from the nearest-neighbor molecules of the solvent or unsolvated formaldehyde and, due to its structure, decompose by a monomolecular mechanism including isomerization[9,12].

2.1 Addition of Free 1-Hydroxyalkyl Radicals with Two or More Carbon Atoms

Free 1-hydroxyalkyl radicals (which result from the abstraction of a hydrogen atom from the carbon atom bonded to the hydroxyl group in molecules of saturated aliphatic alcohols but methanol under the action of chemical initiators[29,30], light[17,31], or ionizing radiation[32,33]) add at the double bond of free formaldehyde dissolved in the alcohol, forming 1,2-alkanediols[8,9,12,29–36], carbonyl compounds, and methanol[8,33] *via* the chaining mechanism. (The yields of the latter two products in the temperature range of 303 to 448 K are one order of magnitude lower.) In these processes, the determining role in the reactivity of the alcohols can be played by the desolvation of formaldehyde in alcohol–formaldehyde solutions, which depends both on the temperature and on the polarity of the solvent[28,33]. For the γ-radiolysis of 1(or 2)-propanol–formaldehyde system at a constant temperature, the dependences of the radiation-chemical yields of 1,2-alkanediols and carbonyl compounds as a function of the formaldehyde concentration show maxima and are symbatic[8,32]. For a constant total formaldehyde concentration of 1 mol dm^{-3}, the dependence of the 1,2-alkanediol yields as a function of temperature for 303–473 K shows a maximum, whereas the yields of carbonyl compounds and methanol increase monotonically[33] (along with the concentration of free formaldehyde[28]). In addition to the above products, the nonchain mechanism in the γ-radiolysis of the solutions of formaldehyde in ethanol and 1- and 2-propanol gives ethanediol, carbon monoxide, and hydrogen in low radiation-chemical yields (which, however, exceed the yields of the same products in the γ-radiolysis of individual alcohols)[8,9,33]. The available experimental data can be described in terms of the following scheme of reactions:

Scheme 2

Chain initiation

1. $I \xrightarrow{2k_1} 2\,R_0^{\bullet}$;

1a. $R_0^{\bullet} + ROH \xrightarrow{k_{1a}} ROH + {}^{\bullet}R_{(-H)}OH$.

Chain propagation

2. ${}^{\bullet}R_{(-H)}OH + CH_2O \xrightarrow{k_2} R_{(-H)}(OH)CH_2O^{\bullet}$;

3. $R_{(-H)}(OH)CH_2O^{\bullet} + ROH \xrightarrow{k_3} R_{(-H)}(OH)CH_2OH + {}^{\bullet}R_{(-H)}O$;

3a. $R_{(-H)}(OH)CH_2O^{\bullet} \xrightarrow{k_{3a}} R_{(-2H)}HO + {}^{\bullet}CH_2OH$
(or $R'R''CO + {}^{\bullet}CH_2OH$);

3b. ${}^{\bullet}CH_2OH + ROH \xrightarrow{k_{3b}} CH_3OH + {}^{\bullet}R_{(-H)}OH$.

Inhibition

4. $R_{(-H)}(OH)CH_2O^{\bullet} + CH_2O \xrightarrow{k_4} R_{(-H)}(OH)CH_2OH + {}^{\bullet}CHO$.

Chain termination

5. $2\,{}^{\bullet}R_{(-H)}OH \xrightarrow{2k_5} R_{(-H)}(OH)R_{(-H)}OH$
(or: $ROH + R_{(-2H)}HO$,
$ROH + R'R''CO$);

6. ${}^{\bullet}R_{(-H)}OH + {}^{\bullet}CHO \xrightarrow{k_6} R_{(-H)}(OH)CHO$
(or: $R_{(-2H)}HO + CH_2O$,
$R'R''CO + CH_2O$, $ROH + CO$);

7. $2\,{}^{\bullet}CHO \xrightarrow{2k_7} HC(O)CHO$
(or: $CH_2O + CO$, $2CO + H_2$).

In these reactions, I is an initiator, e.g., a peroxide[29,30]; $R_0^{\bullet}$, some reactive radical (initiator radical); R, an alkyl; ROH, a saturated aliphatic alcohol, either primary or secondary, beginning from ethanol; CH_2O, the unsaturated molecule – free formaldehyde; $^{\bullet}CH_2OH$, the 1-hydroxymetyl fragment radical; $^{\bullet}R_{(-H)}OH$, the reactive 1-hydroxyalkyl radical (adduct radical), beginning from 1-hydroxyethyl; $^{\bullet}CHO$, the low-reactive formyl radical (inhibitor); R_0H, the molecular product; $R_{(-H)}(OH)CH_2OH$, 1,2-alkanediol; $R_{(-2H)}HO$, an aldehyde in the case of a primary alcohol and an R'R"CO ketone in the case of a secondary alcohol; $R_{(-H)}(OH)R_{(-H)}OH$, a vicinal alkanediol; $R_{(-H)}(OH)CHO$, a hydroxyaldehyde. The chain evolution stage of *Scheme 2* includes consecutive reaction pairs 2–3, 2–3a, and 3a–3b; parallel (competing) reaction pairs 3–3a, 3–3b, 3–4, and 3a–4; and consecutive–parallel reactions 2 and 4.

Scheme 2 does not include the same types of radical-molecule reactions as were considered in Section 1.1 for *Scheme 1*. In addition, it seems unlikely that free adduct radicals will add to formaldehyde at higher temperatures the reaction of adding is unlikely because this would result in an ether bond. The addition of hydroxymethyl radicals to formaldehyde, which is in competition with reaction 3b, is not included as well, because there is no chain formation of ethanediol at 303–448 K[33]. At the same time, small amounts of ethanediol can form *via* the dimerization of a small fraction of hydroxymethyl radicals, but this cannot have any appreciable effect on the overall process kinetics. The addition of free formyl radicals to formaldehyde cannot proceed at a significant rate, as is indicated by the fact that there is no chain formation of glycol aldehyde in the systems examined[33].

The mechanism of the decomposition of the free adduct radical *via* reaction 3a, which includes the formation of an intramolecular H···O bond and isomerization, can be represented as follows[8,9,12]:

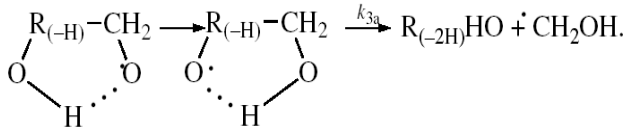

The probability of the occurrence of reaction 3a should increase with increasing temperature. This is indicated by experimental data presented above[8,9,12]. The decomposition of the hydroxyalkoxyl radical. $R_{(-H)}(OH)CH_2O^{\bullet}$ (reaction 3a) is likely endothermic. The endothermic nature of reaction 3a is indirectly indicated by the fact that the decomposition of simple C_2–C_4 alkoxyl radicals $RO^{\bullet}$ in the gas phase is accompanied by heat absorption: (ΔH°_{298} = 30–90 kJ mol^{-1})[2-4]. Reaction 3b, subsequent to reaction 3a, is exothermic, and its heat for C_2–C_3 alcohols in the gas phase is ΔH°_{298} = –40 to –60 kJ mol^{-1}. As follows from the above scheme of the process, reactions 3a and 3b, in which the formation and consumption of the highly reactive free radical hydroxymethyl take place (at equal rates under steady-state conditions), can be represented as a single bimolecular reaction 3a,b occurring in a "cage" of solvent molecules.

The free formyl radical resulting from reaction 4, which is in competition with reactions 3 and 3a, is comparatively low-reactive because its spin density can be partially delocalized from the carbon atom *via* the double bond toward the oxygen atom, which possesses a higher electron affinity[1]. For example, in contrast to the methyl and alkoxyl π-radicals, the formyl σ-radical can be stabilized in glassy alcohols at 77 K[37]. In the gas phase, the dissociation energy of the C–H bond in formyl radicals is half that for acetyl radicals and is about 5 times lower than the dissociation energy of the C_α–H bond in saturated C_1–C_3 alcohols[1].

As distinct from reactions 3 and 3a,b, reaction 4 leads to an inefficient consumption of hydroxyalkoxyl adduct radicals, without regenerating the initial 1-hydroxyalkyl addend radicals. Reaction 4 together with reaction 6 (mutual annihilation of free formyl and chain-carrier 1-hydroxyalkyl radicals) causes the inhibition of the nonbranched-chain process. For the disproportionation of the free radicals, the heats of reactions 5–7 for C_1–C_3 alcohols in the gas phase vary in the range of ΔH°_{298} = –135 to –385 kJ mol^{-1}.[2-4]

The rates of the chain formation of 1,2-alkanediols in reaction 3 (and their nonchain formation in reaction 4), carbonyl compounds in reaction 3a, and methanol in reaction 3b are given by the following equations:

$$V_{3,4}(R_{(-H)}(OH)CH_2OH) = \frac{V_1(\alpha l + x)k_2 x}{k_2 x^2 + (\alpha l + \beta + x)\sqrt{2k_5 V_1}}, \quad (5)$$

$$V_{3a}(R_{(-2H)}HO) = V_{3b}(CH_3OH) = \frac{V_1 \beta k_2 x}{k_2 x^2 + (\alpha l + \beta + x)\sqrt{2k_5 V_1}}, \quad (6)$$

where V_1 is the initiation rate, l is the molar concentration of the saturated alcohol at a given total concentration of formaldehyde[2] dissolved in it, x is the molar concentration of free formaldehyde ($l >> x$), k_2 is the rate constant of reaction 2 (addition of 1-hydroxyalkyl free radical to free formaldehyde), and $\alpha = k_3/k_4$ and $\beta = k_{3a}/k_4$ (mol dm^{-3}) are the ratios of the rate constants of the competing (parallel) reactions. Estimates of $2k_5$ were reported by Silaev *et al*[39,40]. From the extremum condition for the reaction 3a rate function, $\partial V_{3a} / \partial x = 0$, we derived the following analytical expression: $k_2 = (\alpha l_m + \beta)\sqrt{2k_5 V_1} \Big/ x_m^2$.

The overall process rate is a complicated function of the formation and disappearance rates of the $^{\bullet}R_{(-H)}OH$ and $^{\bullet}CHO$ free radicals: $V(R_{(-H)}(OH)CH_2OH, R_{(-2H)}HO, CH_3OH) = V_{1a} + V_3 + V_{3b} - V_4 - V_5 + V_7$. The ratios of the rates of the competing reactions are $V_3/V_4 = \alpha l/x$ and $V_{3a}/V_4 = \beta/x$, and the chain length is $\nu = (V_3 + V_{3a})/V_1$. The ratio of the rates of

[2]The alcohol concentration in alcohol–formaldehyde solutions at any temperature can be estimated by the method suggested in[38,39]. The data necessary for estimating the concentration of free formaldehyde using the total formaldehyde concentration in the solution are reported by Silaev *et al*[28,39].

formation of 1,2-alkanediol and the carbonyl compound is a simple linear function of x:

$V_{3,\ 4}(R_{(-H)}(OH)CH_2OH)/V_{3a}(R_{(-2H)}HO) = (k_4/k_{3a})x + (k_3/k_{3a})l$.

The equations for the rates of chain-termination reactions 5–7 are identical to Eqs. (9)–(11) (see below, Section 3.1).

Figure 2 illustrates the use of Eqs. (5) and (6) for describing the experimental dependences of the formation rates of 1,2-butanediol (curve *1*) in reactions 3 and 4 and propanal (curve *2*) in reaction 3a on the concentration of free formaldehyde in the 1-propanol–formaldehyde reacting system at a total formaldehyde concentration of 2.0 to 9.5 mol dm^{-3} and temperature of 413 K[8,9,41]. The concentration dependence of the propanal formation rate was described using the estimates of kinetic parameters obtained for the same dependence of the 1,2-butanediol formation rate. We considered these data more reliable for the reason that the carbonyl compounds forming in the alcohol–formaldehyde systems can react with the alcohol and this reaction depends considerably on the temperature and acidity of the medium[27]. The mathematical modeling of the process was carried out using a ^{137}Cs γ-radiation dose rate of P = 0.8 Gy s^{-1}[32,41], a total initiation yield of $G(CH_3CH_2\dot{C}HOH)$ = 9.0 particles per 100 eV [8,9] ($V_1 = 4.07 \times 10^{-7}$ mol dm^{-3} s^{-1}), and $2k_5 = 4.7 \times 10^9$ dm^3 mol^{-1} s^{-1}). The following values of the parameters were obtained: $\alpha = 0.36 \pm 0.07$, $\beta = 0.25 \pm 0.05$ mol dm^{-3}, and $k_2 = (6.0 \pm 1.4) \times 10^3$ dm^3 mol^{-1} s^{-1}.

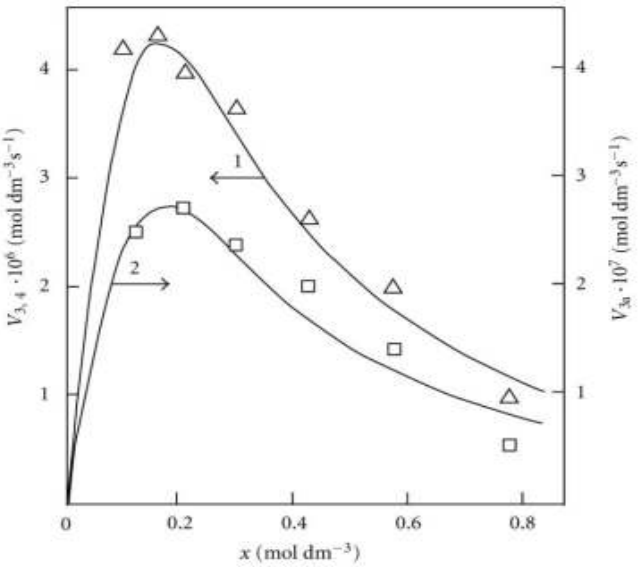

Figure 2: Reconstruction of the functional dependence (curves) of the product formation rates $V_{3,\ 4}$ and V_{3a} on the concentration x of free formaldehyde (model optimization with respect to the parameters α, β and k_2) from empirical data (symbols) for the 1-propanol–formaldehyde system at 413 K [8,9,41]: (*1*, △) calculation using Eq. (5), standard deviation of $S_Y = 2.20 \times 10^{-7}$; (*2*, □) calculation using Eq. (6), $S_Y = 2.38 \times 10^{-8}$.

Note that, as compared to the yields of 1,2-propanediol in the γ-radiolysis of the ethanol–formaldehyde system, the yields of 2,3-butanediol in the γ-radiolysis of the ethanol–acetaldehyde system are one order of magnitude lower[41]. Using data from[8,9], it can be demonstrated that, at 433 K, the double bond of 2-propen-1-ol accepts the 1-hydroxyethyl radical 3.4 times more efficiently than the double bond of formaldehyde[42].

2.2 Addition of the Hydroxymethyl Radical

The addition of hydroxymethyl radicals to the carbon atom at the double bond of free formaldehyde molecules in methanol, initiated by the free-radical mechanism, results in the chain formation of ethanediol[34]. In this case, reaction 3a in Scheme 2 is the reverse of reaction 2, the 1-hydroxyalkyl radical $^{\bullet}R_{(-H)}OH$ is the hydroxymethyl radical $^{\bullet}CH_2OH$, so reaction 3b is eliminated($k_{3b} = 0$), and reaction 5 yields an additional amount of ethanediol *via* the dimerization of chain-carrier hydroxymethyl radicals (their disproportionation can practically be ignored[43]). The scheme of these reactions is presented in[35].

The rate equation for ethanediol formation by the chain mechanism in reaction 3 and by the nonchain mechanism in reactions 4 and 5 in the methanol–formaldehyde system has a complicated form[3] as compared to Eq. (1) for the formation rate of the other 1,2-alkanediols[12]:

$$V_{3,\ 4,\ 5}(CH_2OH)_2 = V_1[f(\alpha l + x)k_2 x + V_1 2k_5(\alpha l + \beta + x)^2]/f^2, \quad (7)$$

where $f = k_2x^2 + (\alpha l + \beta + x)\sqrt{2k_5V_1}$.

If the rate of ethanediol formation by the dimerization mechanism in reaction 5 is ignored for the reason that it is small as compared to the total rate of ethanediol formation in reactions 3 and 4, Eq. (7) will be identical to Eq. (5). After the numerator and denominator on the right-hand side of Eq. (5) are divided by $k_{-2} \equiv k_{3a}$, one can replace k_2 in this equation with $K_2 = k_2/k_{-2}$, which is the equilibrium constant for the reverse of reaction 2. Ignoring the reverse of reaction 2 (k_{3a} = 0, $\beta = 0$) makes Eq. (5) identical to Eq. (4) for *Scheme 1* at k_{3b} = 0 (see the Section 1.1). In this case, the rate constant k_2 is effective.

3. Addition to Oxygen

The addition of a free radical or an atom to one of the two multiply bonded atoms of the oxygen molecule yields a peroxyl free radical and thus initiates oxidation, which is the basic process of chemical evolution. The peroxyl free radical then abstracts the most labile atom from a molecule of the compound being oxidized or decomposes to turn into a molecule of an oxidation product.

The only reaction that can compete with these two reactions at the chain evolution stage is the addition of the peroxyl radical to the oxygen molecule (provided that the oxygen concentration is sufficiently high). This reaction yields a secondary, tetraoxyalkyl, 1:2 adduct radical, which is the heaviest and the largest among the reactants. It is less reactive than the primary, 1:1 peroxyl adduct radical and, as a consequence, does not participate in further chain propagation. At moderate temperatures, the reaction proceeds *via* a nonbranched-chain mechanism.

3.1 Addition of Hydrocarbon Free Radicals

Usually, the convex curve of the hydrocarbon (RH) autooxidation rate as a function of the partial pressure of oxygen ascends up to some limit and then flattens out[6]. When this is the case, the oxidation kinetics is satisfactorily describable in terms of the conventional reaction scheme[2,5,6,16,44,45], which involves two types of free radicals. These are the hydrocarbon radical R$^{\bullet}$ (addend radical) and the

[3]In an earlier publication[8], this equation does not take into account reaction 3a.

addition product $RO_2^{\bullet}$ (1:1 adduct radical). However, the existing mechanisms are inapplicable to the cases in which the rate of initiated oxidation as a function of the oxygen concentration has a maximum (Figs. 3, 4)[46,47]. Such dependences can be described in terms of the competition kinetics of free-radical chain addition, whose reaction scheme involves not only the above two types of free radicals, but also the $RO_4^{\bullet}$ radical (1:2 adduct) inhibiting the chain process[13,14].

Scheme 3

Chain initiation

1. $I \xrightarrow{2k_1} 2R_0^{\bullet}$;

1a. $R_0^{\bullet} + RH \xrightarrow{k_{1a}} R_0H + R^{\bullet}$.

Chain propagation

2. $R^{\bullet} + O_2 \xrightarrow{k_2} RO_2^{\bullet}$;

3. $RO_2^{\bullet} + RH \xrightarrow{k_3} RO_2H + R^{\bullet}$

(or $ROH + RO^{\bullet}$);

3a. $RO_2^{\bullet} \xrightarrow{k_{3a}} R'_{(-H)}HO + R''O^{\bullet}$

(or $R_{(-2H)}HO + {}^{\bullet}OH$);

3b. $R''O^{\bullet}(RO^{\bullet}) + RH \xrightarrow{k_{3b}} R''OH\ (ROH) + R^{\bullet}$

(or ${}^{\bullet}OH + RH \xrightarrow{k_{3b}} H_2O + R^{\bullet}$).

Inhibition

4. $RO_2^{\bullet} + O_2 \xrightarrow{k_4} RO_4^{\bullet}$.

Chain termination

5. $2R^{\bullet} \xrightarrow{2k_5} RR$

(or $R_{(-2H)}H + RH$);

6. $R^{\bullet} + RO_4^{\bullet} \xrightarrow{k_6} RH + R_{(-2H)}HO + O_3$

(or: $ROH + R_{(-2H)}HO + O_2$,

$ROR + O_3$,

$RO_2R + O_2$);

7. $2\,RO_4^{\bullet} \xrightarrow{2k_7} RO_2R + 2O_3$.

The only difference between the kinetic model of oxidation represented by *Scheme 3* and the kinetic model of the chain addition of 1-hydroxyalkyl radicals to the free (unsolvated) form of formaldehyde in nonmethanolic alcohol–formaldehyde systems[8,9] (*Scheme 2*, Section 2.1) is that in the former does not include the formation of the molecular 1:1 adduct *via* reaction 4.

The decomposition of the initiator I in reaction 1 yields a reactive $R_0^{\bullet}$ radical, which turns into the ultimate product R_0H *via* reaction 1a, generating an alkyl radical $R^{\bullet}$, which participates in chain propagation. In reaction 2, the addition of the free radical $R^{\bullet}$ to the oxygen molecule yields a reactive alkylperoxyl 1:1 adduct radical $RO_2^{\bullet}$[45], which possesses increased energy owing to the energy released upon the conversion of the O=O bond into the ordinary bond RO–O$^{\bullet}$ (for addition in the gas phase under standard conditions, this energy is 115–130 kJ mol^{-1} for C_1–C_4 alkyl radicals[1,2,4] and 73 kJ mol^{-1} for the allyl radical[4]). Because of this, the adduct radical can decompose (reaction 3a) or react with some neighbor molecule (reaction 3 or 4) on the spot, without diffusing in the solution and, accordingly, without entering into any chain termination reaction. In reaction 3, the interaction between the radical adduct $RO_2^{\bullet}$ and the hydrocarbon molecule RH yields, *via* a chain mechanism, the alkyl hydroperoxide RO_2H (this reaction regenerates the chain carrier $R^{\bullet}$ and, under certain conditions, can be viewed as being reversible[2]) or the alcohol ROH (this is followed by the regeneration of $R^{\bullet}$ *via* reaction 3b). The latter (alternative) pathway of reaction 3 consists of four steps, namely, the breaking of old bonds and the formation of two new bonds in the reacting structures. In reaction 3a, the isomerization and decomposition of the alkylperoxyl radical adduct $RO_2^{\bullet}$ with O–O and C–O or C–H bond breaking take place[6,44], yielding the carbonyl compound $R'_{(-H)}HO$ or $R_{(-2H)}HO$. Reaction 3b produces the alcohol R″OH or water and regenerates the free radical $R^{\bullet}$ (here, R′ and R″ are radicals having a smaller number of carbon atoms than R). As follows from the above scheme of the process, consecutive reactions 3a and 3b (whose rates are equal within the quasi-steady-state treatment), in which the highly reactive fragment, oxyl radical R″O$^{\bullet}$ (or ${}^{\bullet}OH$) forms and then disappears, respectively, can be represented as a single, combined bimolecular reaction 3a,b occurring in a "cage" of solvent molecules. Likewise, the alternative (parenthesized) pathways of reactions 3 and 3b, which involve the alkoxyl radical $RO^{\bullet}$, can formally be treated as having equal rates. For simple alkyl C_1–C_4 radicals R, the pathway of reaction 3 leading to the alkyl hydroperoxide RO_2H is endothermic (ΔH°_{298} = 30–80 kJ mol^{-1}) and the alternative pathway yielding the alcohol ROH is exothermic (ΔH°_{298}= –120 to –190 kJ mol^{-1}), while the parallel reaction 3a, which yields a carbonyl compound and the alkoxyl radical R″O$^{\bullet}$ or the hydroxyl radical ${}^{\bullet}OH$, is exothermic in both cases (ΔH°_{298} = –80 to –130 kJ mol^{-1}), as also is reaction 3b (ΔH°_{298} = –10 to –120 kJ mol^{-1}), consecutive to reaction 3a, according to thermochemical data for the gas phase[2–4]. In reaction 4, which is competing with (parallel to) reactions 3 and 3a (chain propagation through the reactive radical $R^{\bullet}$), the resulting low-reactive radical that does not participate in further chain propagation and inhibits the chain process is supposed to be

the alkyltetraoxyl 1:2 radical adduct[4,5] $RO_4^{\bullet}$, which has the largest weight and size. This radical is possibly stabilized by a weak intramolecular H···O hydrogen bond[54] shaping it into a six-membered cyclic structure[6] (seven-membered cyclic structure in the case of aromatic and certain branched acyclic hydrocarbons)[56,57]:

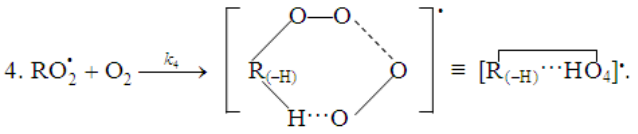

Reaction 4 in the case of the methylperoxyl radical $CH_3O_2^{\bullet}$ adding to the oxygen molecule to yield the methyltetraoxyl radical $CH_3O_4^{\bullet}$ takes place in the gas phase, with heat absorption equal to 110.0 ± 18.6 kJ mol^{-1} (without the energy of the possible formation of a hydrogen bond taken into account). The exothermic reactions 6 and 7, in which the radical R$^{\bullet}$ or $RO_4^{\bullet}$ undergoes disproportionation, include the isomerization and decomposition of the $RO_4^{\bullet}$ radical (taking into account the principle of detailed balance for the various reaction pathways). The latter process is likely accompanied by chemiluminescence typical of hydrocarbon oxidation[52]. These reactions regenerate oxygen as O_2 molecules (including singlet oxygen[7] [52,59] and, partially, as O_3 molecules and yield the carbonyl compound $R_{(-2H)}HO$ (possibly in the triplet excited state[52]). Depending on the decomposition pathway, the other possible products are the alcohol ROH, the ether ROR, and the alkyl peroxide RO_2R. It is likely that the isomerization and decomposition of the $RO_4^{\bullet}$ radical *via* reactions 6 and 7 can take place through the breaking of a C–C bond to yield carbonyl compounds, alcohols, ethers, and organic peroxides containing fewer carbon atoms than the initial hydrocarbon, as in the case of the alkylperoxyl radical $RO_2^{\bullet}$ in reaction 3a. At later stages of oxidation and at sufficiently high temperatures, the resulting aldehydes can be further oxidized into respective carboxylic acids. They can also react with molecular oxygen so that a C–H bond in the aldehyde molecule breaks to yield two free radicals ($HO_2^{\bullet}$ and $^{\bullet}R'_{(-H)}O$ or $^{\bullet}R_{(-2H)}O$). This process, like possible ozone decomposition yielding an $^{\bullet}O^{\bullet}$ atom or peroxide decomposition with O–O bond breaking, leads to degenerate chain branching[6].

The equations describing the formation rates of molecular products at the chain propagation and termination stages of the above reaction scheme, set up using the quasi-steady-state treatment, appear as follows:

$$V_3(RO_2H;\ ROH) = V_1\alpha l k_2 x/f = \quad (8)$$

$$= V_1\alpha l x/f_m\,, \quad (8a)$$

$$V_{3a}(R'_{(-H)}HO;\ R_{(-2H)}HO) = V_{3b}(R''OH;\ H_2O) =$$

$$= V_1\beta\, k_2 x/f = \quad (9)$$

$$= V_1\beta\, x/f_m\,, \quad (9a)$$

$$V_5 = V_1^2 2k_5\left(\alpha l+\beta+x\right)^2/f^2\,, \quad (10)$$

$$2V_6 = 2V_1\sqrt{2k_5V_1}\left(\alpha l+\beta+x\right)k_2x^2/f^2\,, \quad (11)$$

$$V_7 = V_1\left(k_2x^2\right)^2/f^2\,, \quad (12)$$

where V_1 is the initiation rate, l = [RH] and x = [O_2] are the molar concentrations of the starting components ($l >> x$), $\alpha = k_3/k_4$ and $\beta = k_{3a}/k_4$ (mol dm^{-3}) are the ratios of the rate constants of the competing (parallel) reactions, $k_2 = (\alpha l_m+\beta)\sqrt{2k_5V_1}/x_m^2$ is the rate constant of the addition of the alkyl radical R$^{\bullet}$ to the oxygen molecule (reaction 2) as determined by solving the quadratic equation following from the rate function extremum condition $\partial V_{3,3a}/\partial x = 0$, l_m and x_m are the values of l and x at the maximum point of the function, $f = k_2x^2 + (\alpha l+\beta+x)\sqrt{2k_5V_1}$,

and $f_m = x^2 + (\alpha l+\beta+x)x_m^2/(\alpha l_m+\beta)$.

The ratios of the rates of the competing reactions are $V_3/V_4 = \alpha l/x$ and $V_{3a}/V_4 = \beta/x$, and the chain length is $\nu = (V_3 + V_{3a})/V_1$. Eq. (9) is identical to Eq. (6). Eqs (8a) and (9a) were obtained by replacing the rate constant k_2 in Eqs. (8) and (9) with its analytical expression (for reducing the number of unknown parameters to be determined directly).

For $\alpha l >> \beta$ ($V_3 >> V_{3a}$),

when the total yield of alkyl hydroperoxides and alcohols having the same number of carbon atoms as the initial compound far exceeds the yield of carbonyl compounds, as in the case of the oxidation of some hydrocarbons, the parameter β in Eqs. (8) and (8a) can be neglected (β = 0) and these equations become identical to Eqs. (3) and (3a) with the corresponding analytical expression for k_2.

In the alternative kinetic model of oxidation, whose chain termination stage involves, in place of R$^{\bullet}$ (*Scheme 3*), $RO_2^{\bullet}$ radicals reacting with one another and with $RO_4^{\bullet}$ radicals, the

[4]It is hypothesized that raising the oxygen concentration in the *o*-xylene–oxygen system can lead to the formation of the [RO$^{\bullet}$···O_2] intermediate complex[46] similar to the [ROO$^{\bullet}$···(π-bond)RH] complex between the alkylperoxyl 1:1 adduct radical and an unsaturated hydrocarbon suggested in this work. The electronic structure of the π-complexes is considered elsewhere[48].

[5]Thermochemical data are available for some polyoxyl free radicals (the enthalpy of formation of the methyltetraoxyl radical without the energy of the possible intramolecular hydrogen bond H···O taken into account is $\Delta H_f^{\circ}{}_{298}(CH_3O_4^{\bullet})$ = 121.3 ± 15.3 kJ mol^{-1}) and polyoxides ($\Delta H_f^{\circ}{}_{298}(CH_3O_4H)$ = –21.0 ± 9 kJ mol^{-1})[49]. These data were obtained using the group contribution approach. Some physicochemical and geometric parameters were calculated for the methyl hydrotetraoxide molecule as a model compound[50-52]. The IR spectra of dimethyl tetraoxide with isotopically labeled groups in Ar–O_2 matrices were also reported[53]. For reliable determination of the number of oxygen atoms in an oxygen-containing species, it is necessary to use IR and EPR spectroscopy in combination with the isotope tracer method[53].

[6]The $R_{(-H)}H\cdots O(R)O_3$ ring consisting of the same six atoms (C, H, and 4O), presumably with a hydrogen bond[6], also forms in the transition state of the dimerization of primary and secondary alkylperoxyl radicals $RO_2^{\bullet}$ *via* the Russell mechanism[5,55].

[7]Note that the alkylperoxyl radicals $RO_2^{\bullet}$ are effective quenchers of singlet oxygen $O_2(a^1\Delta_g)$[58].

dependences of the chain formation rates of the products on the oxygen concentration x derived by the same method have no maximum: $V_3 = V_1 k_3 l / (k_4 x + \sqrt{2k_5 V_1})$ and $V_{3a} = V_1 k_{3a} / (k_4 x + \sqrt{2k_5 V_1})$. In the kinetic model of oxidation that does not include the competing reaction 4 (k_4 = 0) and involves the radicals $R^{\bullet}$ and $RO_2^{\bullet}$ (the latter instead of $RO_4^{\bullet}$ in *Scheme 3*) in reactions 5–7, the reaction rate functions V_3 and V_{3a} obtained in the same way are fractional rational functions in the form of $a_0 x/(b_0 x + c_0)$, where a_0, b_0, and c_0 are coefficients having no extremum. For a similar kinetic model in which reactions 3a,b and 4 appearing in the above scheme are missing ($k_{3a} = k_4 = 0$), Walling[5], using the quasi-steady-state treatment in the long kinetic chain approximation, when it can be assumed that $V_2 = V_3$, without using the substitution $k_6 = \sqrt{2k_5 2k_7}$ (as distinct from this work)[5,6,16], found that $V_2 = V_3$ is an irrational function of x: $a_1 x / \sqrt{b_1 x^2 + c_1 x + d_1}$ where a_1, b_1, c_1, and d_1 are coefficients. Again, this function has no maximum with respect to the concentration of any of the two components.

Thus, of the three kinetic models of oxidation mathematically analyzed above, which involve the radicals $R^{\bullet}$ and $RO_2^{\bullet}$ in three types of quadratic-law chain termination reactions (reactions 5–7) and are variants of the conventional model[2,5,6,16,44,45], the last two lead to an oxidation rate versus oxygen concentration curve that emanates from the origin of coordinates, is convex upward, and has an asymptote parallel to the abscissa axis. Such monotonic dependences are observed when the oxygen solubility in the liquid is limited under given experimental conditions and the oxygen concentration attained[8] is $[O_2]_{top} \le x_m$.

Unlike the conventional model, the above kinetic model of free-radical nonbranched-chain oxidation, which includes the pairs of competing reactions 3–4 and 3a–4 (*Scheme 3*), allows us to describe the nonmonotonic (peaking) dependence of the oxidation rate on the oxygen concentration (Fig. 3). In this oxidation model, as the oxygen concentration in the binary system is increased, oxygen begins to act as an oxidation autoinhibitor or an antioxidant *via* the further oxidation of the alkylperoxyl 1:1 adduct radical $RO_2^{\bullet}$ into the low-reactive 1:2 adduct radical $RO_4^{\bullet}$ (reactions 4 and 6 lead to inefficient consumption of the free radicals $RO_2^{\bullet}$ and $R^{\bullet}$ and cause shortening of the kinetic chains). The optimum oxygen concentration x_m, at which the oxidation rate is the highest, can be calculated using kinetic equations (8a) and (9a) and Eq. (3a) with $\beta = 0$ or the corresponding analytical expression for k_2. In the familiar monograph *Chain Reactions* by Semenov [60], it is noted that raising the oxygen concentration when it is already sufficient usually slows down the oxidation process by shortening the chains. The existence of the upper (second) ignition limit in oxidation is due to chain termination in the bulk through triple collisions between an active species of the chain reaction and two oxygen molecules (at sufficiently high oxygen partial pressures). In the gas phase at atmospheric pressure, the number of triple collisions is roughly estimated to be 10^3 times smaller than the number of binary collisions (and the probability of a reaction taking place depends on the specificity of the action of the third particle).

Curve *1* in Fig. 3 illustrates the fit between Eq. (3a) at $\alpha l >> \beta$ and experimental data for the radiation-induced oxidation of *o*-xylene in the liquid phase at 373 K in the case of 2-methylbenzyl hydroperoxide forming much more rapidly than *o*-tolualdehyde ($V_3 >> V_{3a}$ and $\alpha l >> \beta$)[46]. The oxygen concentration limit in *o*-xylene is reached at an oxygen concentration of $[O_2]_{top} > x_m$, which corresponds to the third experimental point[46]. The oxygen concentration was calculated from the oxygen solubility in liquid xylene at 373 K[61]. The following quantities were used in this mathematical description: ^{60}Co γ-radiation dose rate of P = 2.18 Gy s^{-1} and total initiation yield of $G(o\text{-}CH_3C_6H_4\dot{C}H_2)$ = 2.6 particles per 100 eV of the energy absorbed by the solution[46]; $V_1 = 4.73 \times 10^{-7}$ mol dm^{-3} s^{-1}, and $2k_5 = 1.15 \times 10^{10}$ dm^3 mol^{-1} s^{-1}. The resulting value of the parameter α is $(9.0 \pm 1.8) \times 10^{-3}$; hence, $k_2 = (3.2 \pm 0.8) \times 10^5$ dm^3 mol^{-1} s^{-1}. From the data presented in [62], it was estimated that $k_4 = k_3/\alpha = (5.2 \pm 1.2) \times 10^2$ dm^3 mol^{-1} s^{-1}.

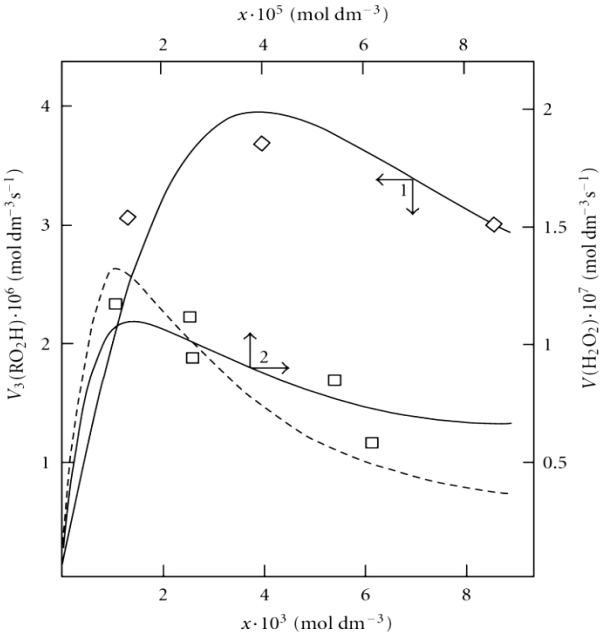

Figure 3: (*1*, ◇) Reconstruction of the functional dependence of the 2-methylbenzyl hydroperoxide formation rate $V_3(RO_2H)$ on the dissolved oxygen concentration x from empirical data (points) using Eq. (3a) (model optimization with respect to the parameter α) for the *o*-xylene–oxygen system at 373 K [46] (standard deviation of $S_Y = 5.37 \times 10^{-7}$. (*2*, □) Reconstruction of the functional dependence of the total hydrogen peroxide formation rate $V_{3,7}(H_2O_2)$ on the dissolved oxygen concentration x from empirical data (symbols) using Eqs. (3a) and (12) with $\beta = 0$ (model optimization with respect to the parameter α) for the γ-radiolysis of water saturated with hydrogen and containing different amounts of oxygen at 296 K [63] ($S_Y = 1.13 \times 10^{-8}$). The dashed curve described

[8]The oxygen concentration attained in the liquid may be below the thermodynamically equilibrium oxygen concentration because of diffusion limitations hampering the establishment of the gas–liquid saturated solution equilibrium under given experimental conditions (for example, when the gas is bubbled through the liquid) or because the Henry law is violated for the given gas–liquid system under real conditions.

$V_3(H_2O_2)$ as a function of the oxygen concentration x based on Eq. (3a) (model optimization with respect to α) and the experimental data of curve *2* ($S_Y = 1.73 \times 10^{-8}$).

3.2 Addition of the Hydrogen Atom

A number of experimental findings concerning the autoinhibiting effect of an increasing oxygen concentration at modest temperatures on hydrogen oxidation both in the gas phase[47,64,65] (Fig. 4) and in the liquid phase[63] (Fig. 3, curve *2*), considered in our earlier work[66], can also be explained in terms of the competition kinetics of free radical addition[14,67].

Scheme 4

Nonbranched-chain oxidation of hydrogen and changes in enthalpy (ΔH°_{298}, kJ mol^{-1}) for elementary reactions[9]

Chain initiation

1. $H_2 \xrightarrow{h\nu,\,\gamma} 2H^\bullet$, $\Delta H^\circ_{298} = 436.0 \pm 0.0$.

Chain propagation

2. $H^\bullet + O_2 \xrightarrow{k_2} HO_2^\bullet$, $\Delta H^\circ_{298} = -205.4 \pm 1.7$;

3. $HO_2^\bullet + H_2 \xrightarrow{k_3} H_2O + HO^\bullet$, $\Delta H^\circ_{298} = -215.4 \pm 2.9$

(or $H_2O_2 + H^\bullet$), $\Delta H^\circ_{298} = 69.4 \pm 1.7$;

3′. $HO^\bullet + H_2 \xrightarrow{k_{3'}} H_2O + H^\bullet$, $\Delta H^\circ_{298} = -62.8 \pm 1.2$.

Inhibition

4. $HO_2^\bullet + O_2 \xrightarrow{k_4} HO_4^\bullet$, $\Delta H^\circ_{298} = 110.0 \pm 15.4$.

Chain termination

5. $2H^\bullet (+M) \xrightarrow{2k_5} H_2 (+M)$, $\Delta H^\circ_{298} = -436.0 \pm 0.0$;

6. $H^\bullet + HO_4^\bullet \xrightarrow{k_6} H_2O_2 + O_2$, $\Delta H^\circ_{298} = -476.6 \pm 13.7$

(or: $H_2O + O_3$, $\Delta H^\circ_{298} = -439.3 \pm 15.4$,

$H_2 + 2O_2$), $\Delta H^\circ_{298} = -340.6 \pm 13.7$;

7. $2\,HO_4^\bullet \xrightarrow{2k_7} H_2O_2 + 2O_3$, $\Delta H^\circ_{298} = -95.0 \pm 30.8$.

[9]According to Francisco and Williams[49], the enthalpy of formation ($\Delta H_f^\circ{}_{298}$) in the gas phase of $H^\bullet$, $HO^\bullet$, $HO_2^\bullet$, $HO_4^\bullet$ (the latter without the possible intramolecular hydrogen bond taken into account), O_3, H_2O [2], H_2O_2, and H_2O_4 is 218.0 ± 0.0, 39.0 ± 1.2, 12.6 ± 1 $HO_2^\bullet$ .7, 122.6 ± 13.7, 143.1 ± 1.7, –241.8 ± 0.0, –136.0 ± 0, and –26.0 ± 9 kJ mol^{-1}, respectively. Calculations for the $HO_4^\bullet$ radical with a helical structure were carried out using the G2(MP2) method[68]. The stabilization energies of $HO_2^\bullet$, $HO_4^\bullet$, and $HO_3^\bullet$ were calculated in the same work to be 64.5 ± 0.1, 69.5 ± 0.8, and 88.5 ± 0.8 kJ mol^{-1}, respectively. The types of the O_4 molecular dimers, their IR spectra, and higher oxygen oligomers were reported[69,70]. The structure and IR spectrum of the hypothetical cyclotetraoxygen molecule O_4, a species with a high energy density, were calculated by the CCSD method, and its enthalpy of formation was estimated[71]. The photochemical properties of O_4 and the van der Waals nature of the O_2–O_2 bond were investigated[72,73]. The most stable geometry of the dimer is two O_2 molecules parallel to one another. The O_4 molecule was identified by NR mass spectrometry[74].

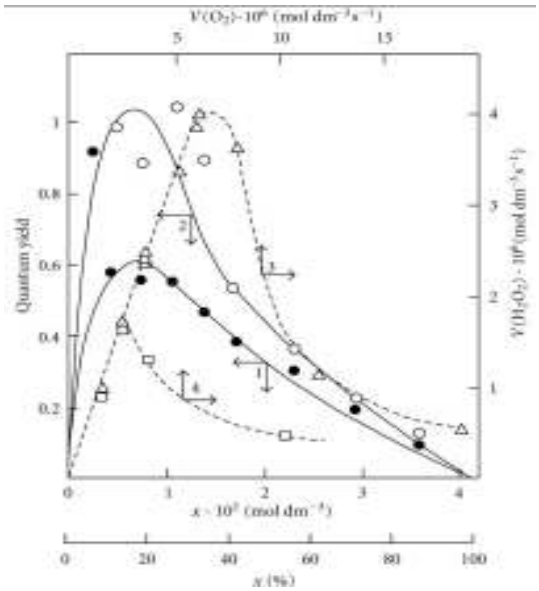

Figure 4: (*1*, *2*) Quantum yields of (*1*, ●) hydrogen peroxide and (*2*, ○) water resulting from the photochemical oxidation of hydrogen in the hydrogen–oxygen system as a function of the oxygen concentration x (light wavelength of 171.9–172.5 nm, total pressure of 10^5 Pa, room temperature [64]). (*3*, *4*) Hydrogen peroxide formation rate $V(H_2O_2)$ (dashed curves) as a function of the rate $V(H_2O_2)$ at which molecular oxygen is passed through a gas-discharge tube filled with (*3*, △) atomic and (*4*, □) molecular hydrogen. Atomic hydrogen was obtained from molecular hydrogen in the gas-discharge tube before the measurements (total pressure of 25–77 Pa, temperature of 77 K [47]). The symbols represent experimental data.

The hydroperoxyl free radical $HO_2^\bullet$ resulting from[75-78] reaction 2 possesses an increased energy due to the energy released the conversion of the O=O multiple bond into the HO–O$^\bullet$ ordinary bond. Therefore, before its possible decomposition, it can interact with a hydrogen or oxygen molecule as the third body *via* parallel (competing) reactions 3 and 4, respectively. The hydroxyl radical $HO^\bullet$ that appears and disappears in consecutive parallel reactions 3 (first variant) and 3′ possesses additional energy owing to the exothermicity of the first variant of reaction 3, whose heat is distributed between the two products. As a consequence, this radical has a sufficiently high reactivity not to accumulate in the system during these reactions, whose rates are equal ($V_3 = V_{3'}$) under quasi-steady-state conditions, according to the above scheme. Parallel reactions 3 (second, parenthesized variant) and 3′ regenerate hydrogen atoms. It is assumed[56,57] that the hydrotetraoxyl radical $HO_4^\bullet$ (first reported in[79,80]) resulting from endothermic reaction 4, which is responsible for the peak in the experimental rate curve (Fig. 2, curve *3*), is closed into a five-membered $[\overline{OO{-}H\cdots OO}]^\bullet$ cycle due to weak intramolecular hydrogen bonding[54,81]. This structure imparts additional stability to this radical and makes it least reactive. The $HO_4^\bullet$ radical was discovered by Staehelin *et al*[82]. in a pulsed radiolysis study of ozone degradation in water; its UV spectrum with an absorption maximum at 260 nm ($\varepsilon(HO_4^\bullet)_{280\ nm}$ = 320 ±15 m^2 mol^{-1}) was reported. The spectrum of the $HO_4^\bullet$ radical is similar to that of ozone, but

the molar absorption coefficient $\varepsilon(HO_4^{\bullet})_{\lambda_{max}}$ of the former is almost two times larger 82]. The assumption about the cyclic structure of the $HO_4^{\bullet}$ radical can stem from the fact that its mean lifetime in water at 294 K, which is (3.6 ± 0.4) × 10^{-5} s (as estimated[66] from the value of $1/k$ for the reaction $HO_4^{\bullet} \xrightarrow{k} HO_2^{\bullet} + O_2$)[82], is 3.9 times longer than that of the linear $HO_3^{\bullet}$ radical[68, 83] estimated in the same way[66] for the same conditions[84], (9.1 ± 0.9) × 10^{-6} s. MP2/6-311++G** calculations using the Gaussian-98 program confirmed that the cyclic structure[85] of $HO_4^{\bullet}$ is energetically more favorable than the helical structure[68] (the difference in energy is 4.8–7.3 kJ mol^{-1}, depending on the computational method and the basis set).[10] For example, with the MP2(full)/6-31G(d) method, the difference between the full energies of the cyclic and acyclic $HO_4^{\bullet}$ conformers with their zero-point energies (ZPE) values taken into account (which reduces the energy difference by 1.1 kJ mol^{-1}) is –5.1 kJ mol^{-1} and the entropy of the acyclic-to-cyclic $HO_4^{\bullet}$ transition is ΔS°_{298} = –1.6 kJ mol^{-1} K^{-1}. Therefore, under standard conditions, $HO_4^{\bullet}$ can exist in both forms, but the cyclic structure is obviously dominant (87%, K_{eq} = 6.5) [85].

Reaction 4 and, to a much lesser degree, reaction 6 inhibit the chain process, because they lead to inefficient consumption of its main participants – $HO_2^{\bullet}$ and $H^{\bullet}$.

The hydrogen molecule that results from reaction 5 in the gas bulk possesses an excess energy, and, to acquire stability within the approximation used in this work, it should have time for deactivation *via* collision with a particle M capable of accepting the excess energy[87]. To simplify the form of the kinetic equations, it was assumed that the rate of the bimolecular deactivation of the molecule substantially exceeds the rate of its monomolecular decomposition, which is the reverse of reaction 5 [2].

Reactions 6 and 7 (taking into account the principle of detailed balance for the various pathways) regenerate hydrogen and oxygen (in the form of $O_2(X^3\Sigma_g^-)$ molecules, including the singlet states[49,70] with $\Delta H^{\circ}_{f298}(O_2, a^1\Delta_g)$ = 94.3 kJ mol^{-1}] and $\Delta H^{\circ}_{f298}(O_2, b^1\Sigma_g^+)$ = 161.4 kJ mol^{-1}, which are deactivated by collisions, and in the form of O_3) and yield hydrogen peroxide or water *via* a nonchain mechanism, presumably through the intermediate formation of the unstable hydrogen tetraoxide molecule H_2O_4 [88].[11] Ozone does not interact with molecular hydrogen. At moderate temperatures, it decomposes fairly slowly, particularly in the presence of $O_2(X^3\Sigma_g^-)$[70]. The reaction of ozone with $H^{\bullet}$ atoms, which is not impossible, results in their replacement with $HO^{\bullet}$ radicals. The relative contributions from reactions 6 and 7 to the process kinetics can be roughly estimated from the corresponding enthalpy increments (*Scheme 4*).

When there is no excess hydrogen in the hydrogen–oxygen system and the homomolecular[71-74,89,90] dimer O_4, which exists at low concentrations (depending on the pressure and temperature) in equilibrium with O_2 [70], can directly capture the $H^{\bullet}$ atom to yield the heteronuclear cluster $HO_4^{\bullet}$,[12] which is more stable than O_4 [70] and cannot abstract a hydrogen atom from the hydrogen molecule, nonchain hydrogen oxidation will occur to give molecular oxidation products *via* the disproportionation of free radicals.

The low-reactive hydrotetraoxyl radical[82] $HO_4^{\bullet}$, which presumably has a high energy density[71], may be an intermediate in the efficient absorption and conversion of biologically hazardous UV radiation energy the Earth upper atmosphere. The potential energy surface for the atmospheric reaction $HO^{\bullet} + O_3$, in which the adduct $HO_4^{\bullet}$ (^2A) was considered as an intermediate, was calculated by the DMBE method[91]. From this standpoint, the following reactions are possible in the upper troposphere, as well as in the lower and middle stratosphere, where most of the ozone layer is situated (altitude of 16–30 km, temperature of 217–227 K, pressure of 1.0 × 10^4–1.2 × 10^3 Pa[92]; the corresponding ΔH°_{298} reaction values are given in kJ mol^{-1})[49]:

$$H_2O(\text{vapor}) + h\nu \rightarrow H^{\bullet} + HO^{\bullet}; \quad (8)$$

$$HO^{\bullet} + O_3 \rightarrow HO_4^{\bullet}\ [80,82,91], \quad \Delta H^{\circ}_{298} = -59.5; \quad (9)$$

$$HO_4^{\bullet} \rightarrow HO_2^{\bullet} + O_2(X^3\Sigma_g^-)\ [82,91], \quad \Delta H^{\circ}_{298} = -110.0 \quad (10)$$

$$(\text{or } HO_2^{\bullet} + O_2(a^1\Delta_g), \quad \Delta H^{\circ}_{298} = -15.7.$$

The $HO_4^{\bullet}$ radical can disappear *via* disproportionation with a molecule, free radical, or atom in addition to dissociation. Note that emission from $O_2(a^1\Delta_g)$ and $O_2(b^1\Sigma_g^+)$ is observed at altitudes of 30–80 and 40–130 km, respectively[93].

Staehelin *et al*[82]. pointed out that, in natural systems in which the concentrations of intermediates are often very low, kinetic

[10]There were calculations for the two conformers (*cis* and *trans)* of the $HO_4^{\bullet}$ radical[86] using large scale *ab initio* methods and density functional techniques with extended basis sets. Both conformers have a nearly planar geometry with respect to the four oxygen atoms and present an unusually long central O–O bond. The most stable conformer of $HO_4^{\bullet}$ radical is the *cis* one, which is computed to be endothermic with respect to $HO_2^{\bullet}(X^2A'') + O_2(X^3\Sigma_g^-)$ at 0 K.

[11]The planar, six-atom, cyclic, hydrogen-bonded dimer $(HO_2^{\bullet})_2$ was calculated using quantum chemical methods (B3LYP density functional theory)[88]. The hydrogen bond energy is 47.7 and 49.4 kJ mol^{-1} at 298 K for the triplet and singlet states of the dimer, respectively.

[12]It is impossible to make a sharp distinction between the two-step bimolecular interaction of three species via the equilibrium formation of the labile intermediate O_4 and the elementary trimolecular reaction $O_2 + O_2 + H^{\bullet} \rightarrow HO_4^{\bullet}$.

chains in chain reactions can be very long in the absence of scavengers since the rates of the chain termination reactions decrease with decreasing concentrations of the intermediates according to a quadratic law, whereas the rates of the chain propagation reactions decrease according to a linear law.

The kinetic description of the noncatalytic oxidation of hydrogen, including in an inert medium[87]], in terms of the simplified scheme of free-radical nonbranched-chain reactions (*Scheme 4*), which considers only quadratic-law chain termination and ignores the surface effects[47], at moderate temperatures and pressures, in the absence of transitions to unsteady-state critical regimes, and at a substantial excess of the hydrogen concentration over the oxygen concentration was obtained by means of quasi-steady-state treatment, as in the previous studies on the kinetics of the branched-chain free-radical oxidation of hydrogen[76], even though the applicability of this method in the latter case under unsteady states conditions was insufficiently substantiated. The method was used with the following condition:[13] $k_6 = \sqrt{2k_5 2k_7}$ (see Introduction). The equation for the rate of the chain formation of hydrogen peroxide and water, $V_3(H_2O_2; H_2O) = V_{3'}(H_2O)$, *via* reactions 3 and 3′ is identical to Eq. (3, 3a) with the corresponding analytical expression for k_2. The ratio of the rates of the competing reactions is $V_3/V_4 = \alpha l/x$, and the chain length is $\nu = V_3/V_1$. The rates of nonchain formation of hydrogen peroxide and water *via* reactions (6) and (7) – quadratic-law chain termination – are identical to Eqs. (11) and (12) provided that $\beta = 0$. In these equations, l and x are the molar concentrations of hydrogen and oxygen ($l >> x$), l_m and x_m are the respective concentrations at the maximum point of the function, V_1 is the rate of initiation (reaction 1), $\alpha = k_3/k_4$, the rate constant $k_2 = \alpha l_m \sqrt{2k_5 V_1}/x_m^2$ is derived from the condition $\partial V_3/\partial x = 0$, and $2k_5$ is the rate constant of reaction 5 (hydrogen atom recombination), which is considered as bimolecular within the given approximation.[14]

In the case of nonchain hydrogen oxidation *via* the above addition reaction ($H^{\bullet} + O_4 \xrightarrow{k_{add}} HO_4^{\bullet}$), the formation rates of the molecular oxidation products in reactions 6 and 7 (*Scheme 4*, $k_2 = k_3 = k_4 = 0$) are defined by modified Eqs. (11) and (12) in which $\beta = 0$, $(\alpha l + x)$ is replaced with 1, and k_2 is replaced with $k_{add}K_{eq}$ ($k_{add}K_{eq}$ is the effective rate constant of $H^{\bullet}$ addition to the O_4 dimer, $K_{eq} = k/k'$ is the equilibrium constant of the reversible reaction $2O_2 \underset{k'}{\overset{k}{\Leftrightarrow}} O_4$ with $k' >>$ $k_{add}[H^{\bullet}]$). The formation rates of the stable products of nonchain oxidation ($k_3 = 0$), provided that either reactions (2) and (4) or reaction (2) alone ($k_4 = 0$) occurs (*Scheme 4*; in the latter case, reactions 6 and 7 involve the $HO_2^{\bullet}$ radical rather than $HO_4^{\bullet}$), are given by modified Eqs. (11) and (12) with $\beta = 0$, $(\alpha l + x)$ replaced with 1, and x^2 replaced with x.

Note that, if in *Scheme 4* chain initiation *via* reaction 1 is due to the interaction between molecular hydrogen and molecular oxygen yielding the hydroxyl radical $HO^{\bullet}$ instead of $H^{\bullet}$ atoms and if this radical reacts with an oxygen molecule (reaction 4) to form the hydrotrioxyl radical $HO_2^{\bullet}$ (which was obtained in the gas phase by neutralization reionization (NR) mass spectrometry[83] and has a lifetime of $>10^{-6}$ s at 298 K) and chain termination takes place *via* reactions 5–7 involving the $HO^{\bullet}$ and $HO_3^{\bullet}$, radicals instead of $H^{\bullet}$ and $HO_4^{\bullet}$, respectively, the expressions for the water chain formation rates derived in the same way will appear as a rational function of the oxygen concentration x without a maximum: $V_{3'}(H_2O) = V_1 k_{3'} l/(k_4 x + \sqrt{2k_5 V_1})$.

Curve *2* in Fig. 3 describes, in terms of the overall equation $V_{3,7} = V_1 x(\alpha l f_m + x^3)/f_m^2$ for the rates of reactions 3 and 7 (which was derived from Eqs. 3a and 12, respectively, the latter in the form of $V_7 = V_1 x^4/f_m^2$ (12a) [96]] in which k_2 is replaced with its analytical expression derived from Eq. (8) with $\beta = 0$ everywhere), the dependence of the hydrogen peroxide formation rate (minus the rate $V_{H_2O_2} = 5.19 \times 10^{-8}$ mol dm^{-3} s^{-1} of the primary formation of hydrogen peroxide after completion of the reactions in spurs) on the initial concentration of dissolved oxygen during the γ-radiolysis of water saturated with hydrogen (7×10^{-4} mol dm^{-3}) at 296 K [63]. These data were calculated in the present work from the initial slopes of hydrogen peroxide buildup versus dose curves for a ^{60}Co γ-radiation dose rate of $P = 0.67$ Gy s^{-1} and absorbed doses of $D \cong 22.5$–304.0 Gy. The following values of the primary radiation-chemical yield G (species per 100 eV of energy absorbed) for water γ-radiolysis products in the bulk of solution at pH 4–9 and room temperature were used (taking into account that $V = GP$ and $V_1 = G_H P$): $G_{H_2O_2} = 0.75$ and $G_H = 0.6$ (initiation yield; see below)[94]; $V_1 = 4.15 \times 10^{-8}$ mol dm^{-3} s^{-1}; $2k_5 = 2.0 \times 10^{10}$ dm^3 mol^{-1} s^{-1}. As can be seen from Fig. 3, the best description of the data with an increase in the oxygen concentration in water is attained when the rate V_7 of the formation of hydrogen peroxide *via* the nonchain mechanism in the chain termination reaction 7 (curve *1*, $\alpha = (8.5 \pm 2) \times 10^{-2}$) is taken into account in addition to the rate V_3 of the chain formation of this product *via* the propagation reaction 3 (dashed curve *2*, $\alpha = 0.11 \pm 0.026$). The rate constant of addition reaction 2 determined from α is substantially underestimated: $k_2 = 1.34 \times 10^7$ (*vs* 2.0×10^{10})[94] dm^3 mol^{-1} s^{-1}. The difference can be due to the fact that the radiation-chemical specifics of the process were not considered in the kinetic description of the experimental data. These include oxygen consumption *via* reactions that are not involved in the

[13]For example, the ratio of the rate constants of the bimolecular disproportionation and dimerization of free radicals at room temperature is $k(HO^{\bullet} + HO_2^{\bullet})/[2k(2HO^{\bullet})2k(2HO_2^{\bullet})]^{0.5} = 2.8$ in the atmosphere[92] and $k(H^{\bullet} + HO^{\bullet})/[2k(2H^{\bullet})2k(2HO^{\bullet})]^{0.5} = 1.5$ in water[94]. These values that are fairly close to unity.

[14]This rate constant in the case of the pulsed radiolysis of ammonia–oxygen (+ argon) gaseous mixtures at a total pressure of 10^5 Pa and a temperature of 349 K was calculated to be 1.6×10^8 dm^3 mol^{-1} s^{-1} [65] (a similar value of this constant for the gas phase was reported in an earlier publication[95]). Pagsberg *et al.*[65] found that the dependence of the yield of the intermediate $HO^{\bullet}$ on the oxygen concentration has a maximum close to 5×10^{-4} mol dm^{-3}. In the computer simulation of the process, they considered the strongly exothermic reaction $HO_2^{\bullet} + NH_3 \rightarrow H_2O + {}^{\bullet}NHOH$, which is similar to reaction 3 in *Scheme 4*, whereas the competing reaction 4 was not taken into account.

hydrogen oxidation scheme[66,97,98] and reverse reactions resulting in the decomposition of hydrogen peroxide by intermediate products of water radiolysis (e^-_{aq}, H$^\bullet$, HO$^\bullet$), with the major role played by the hydrated electron[94].

5. General Scheme of the Addition of Free Saturated Radicals to C=C, C=O, and O=O Bonds of Molecules

The general scheme of the nonbranched-chain addition of a free radical from a saturated compound to an olefin (and its functionalized derivative), formaldehyde, or dioxygen in liquid homogeneous binary systems of these components includes the following reactions[57,97,98].

Scheme 5

Initiation

1. $I \xrightarrow{2k_1} 2R^\bullet_0$;

1a. $R^\bullet_0 + R_1A \xrightarrow{k_{1a}} R_0A + R^\bullet_1$;

for addition to an olefin at comparable component concentrations,

1b. $R^\bullet_0 + R_2B \xrightarrow{k_{1b}} R_0B + R^\bullet_2$.

Chain propagation

2. $R^\bullet_1 + R_2B \xrightarrow{k_2} R^\bullet_3$;

3. $R^\bullet_3 + R_1A \xrightarrow{k_3} R_3A + R^\bullet_1$;

for addition to O_2 and the 1-hydroxyalkyl radical to CH_2O,

3a. $R^\bullet_3 \xrightarrow{k_{3a}} R'R''CO + R^\bullet_4$;

3b. $R^\bullet_4 + R_1A \xrightarrow{k_{3b}} R_4A + R^\bullet_1$.

Inhibition

For addition to an olefin or CH_2O,

4. $R^\bullet_3 + R_2B \xrightarrow{k_4} R_3B + R^\bullet_2$;

for addition to O_2,

4a. $R^\bullet_3 + R_2B \xrightarrow{k_{4a}} R^\bullet_{2a}$.

Chain termination

5. $2R^\bullet_1 \xrightarrow{2k_5} Prod$;

6. $R^\bullet_1 + R^\bullet_{2(2a)} \xrightarrow{k_6} Prod$;

7. $2R^\bullet_{2(2a)} \xrightarrow{2k_7} Prod$.

In this scheme, I is the initiator, for example, a peroxide[5,17,18,29,30]; $R^\bullet_0$ is any reactive radical (initiator); A is an atom of hydrogen[2,5,6,17,18,22–24,29–32] or halogen[2,5,19–21]; B is an atom of hydrogen [5,17–21,23,24, 29–32], halogen[22], or oxygen (in oxidation)[2,5 6,16,44–46]; $R^\bullet_1$ is a radical such as $^\bullet PCl_2$, $^\bullet CCl_3$, an alkyl[2,5,6,19-21], a 1-hydroxyalkyl[5,6,17,22–24,29,32], or a similar functionalized radical[5] (addend); $R^\bullet_2$ is the formyl [8,9,29], an alkenyl (propenyl or higher)[2,5,17–22], a 1-hydroxyalkenyl[5,17,18,23,24], or a similar functionalized low-reacrtive radical[5,18] (inhbitor) or the oxygen atom (in oxidation)[2,5,6,13,14,16,44–46,56,57,96–98]; $R^\bullet_{2a}$ is the low-reactive alkyltetraoxyl 1:2 adduct radical $RO^\bullet_4$ [13,14,56,57,96–98] (inhibitor); $R^\bullet_3$ is the active 1:1 adduct radical; $R^\bullet_4$ is an active fragment radical, such as hydroxymethyl[8,9,12,29,32], an alkoxyl radical, or hydroxyl (in oxidation)[2,5,6,13,14,16,44,46,56,57,96–98]; R_0A, R_0B, R_1A, and R_4A are saturated molecules; R_2B is an unsaturated molecule, viz., an olefin[2,5,11,17–22], formaldehyde[8,9,12,29–32], or dioxygen (in oxidation)[2,5,6,13,14,16,44–46,56,57,96–98]; R′R″CO is a carbonyl compound viz., aldehyde [2,6,8,9,12,14,29–32,44] or ketone[2,6,14,29,32,44]; R_3A and R_3B are molecular products (1:1 adducts); and Prod stands for molecular products of the dimerization and disproportionation of free radicals.

The chain evolution stage of *Scheme 5* include consecutive reactions 2, 3; 2, 3a; and 3a, 3b; parallel (competitive) reactions 3, 3a; 3, 3b; 3, 4 (or 4a); and 3a, 4 (or 4a); and consecutive-parallel reactions 2 and 4 (or 4a). Addition to olefins is described by reactions 1–3, 4, and 5–7 and the corresponding rate equations (1)–(4a). Addition to the carbonyl carbon atom of the free (unsolvated) form of formaldehyde is represented by reactions 1, 1a, 2–4 (the main products are a 1,2-alkanediol, a carbonyl compound, and methanol), and 5–7 and is described by Eqs. (5) and (6). In the case of hydroxymethyl addition, the process includes reactions 1, 1a, 2, 3, 5a, 4 (the main product is ethanediol), and 5–7 and is described by Eq. (7). If the nonchain formation of ethanediol in reaction 5 is ignored, the process is described by Eq. (5). Addition to the oxygen molecule is described by reactions 1, 1a, 2–3b, 4a (the main products are an alkyl hydroperoxide, alcohols, carbonyl compounds, and water), and 5–7 and Eqs. (8), (8a), (9), and (9a).

The main molecular products of the chain process – R_3A, R′R″CO, and R_4A – result from reactions 3, 3a, and 3b – chain propagation through the reactive free radical $R^\bullet_1$ or $R^\bullet_4$, R′R″CO. The competing reaction 4, which opposes this chain propagation, yields the by-product R_3B a nonchain mechanism. The rate of formation of the products is a complicated function of the formation rates ($V_{3a} = V_{3b}$) and disappearance rates of the free radicals $R^\bullet_1$ and $R^\bullet_{2(2a)}$: $V(R_3A, R'R''CO, R_4A, R_3B) = V_2 = V_3 + V_{3a} + V_{4(4a)} = (V_{1a} + V_3 + V_{3b} - V_5) - (V_{1b} + V_{4(4a)} - V_7)$. The rates of reactions 5–7 at $k_{1b} = 0$ ($[R_1A] >> [R_2B]$) are given by Eqs. (9)–(11). The rate ratios of the competing reactions are $V_3/V_{4(4a)} = \alpha l/x$ and $V_{3a}/V_{4(4a)} = \beta/x$ (where $\alpha = k_3/k_{4(4a)}$, $\beta = k_{3a}/k_{4(4a)}$ mol dm^{-3}, and l and x are the molar concentrations of the reactants R_1A and

R_2B, respectively), and the chain length is $\nu = (V_3 + V_{3a})/V_1$. Unlike the dependences of the rates of reactions 4a (or 4 at $k_{1b} = 0$, with $V_{4(4a)} \leq V_1$), 5, and 7 (Eqs. (9), (10), and (12)), the dependences of the rates V of reactions 3, 3a,b, 4 (at $k_{1b} \neq 0$), and 6 (Eqs. (1)–(9a) and (11)) on x have a maximum. Reaction 1b, which competes with reaction 1a, gives rise to a maximum in the dependence described by Eq. (2), whereas reaction 4 or 4a, competing with reactions 3 and 3a,b, is responsible for the maxima in the dependences defined by Eqs. (1), (3)–(7) or (8, 8a) and (9, 9a). The low-reactive radicals $R_2^{\bullet}$ [15] and $R_{2a}^{\bullet}$, resulting from reactions 4 and 4a, inhibit the nonbranched-chain addition of $R_1^{\bullet}$ to olefins (or formaldehyde) and dioxygen, respectively. Reaction 4a leads to non-productive loss of $R_3^{\bullet}$ adduct radicals.

For approximate estimation of the parameters of the kinetic equations (3), (4), (8), and (9), Eq. (4) under the conditions (a) $k_2x^2 << (\alpha l + x)\sqrt{2k_5V_1}$ (ascending branch of a peaked curve) and (b) $k_2x^2 >> (\alpha l + x)\sqrt{2k_5V_1}$ (descending branch) is transformed into simple functions (direct and inverse proportionality, respectively) of the concentration x of the unsaturated compound. These functions allow tentative estimates of the parameters k_2 and α to be derived from the experimental product formation rate V provided that V_1 and $2k_5$ are known:

$$V_{3,4} = \sqrt{V_1}k_2x/\phi\sqrt{2k_5}, \quad (13)$$

$$V_{3,4} = (V_1/\varphi)[(\alpha l/x) + 1], \quad (14)$$

where $\varphi = 1$ under conditions (a) and (b) and $\varphi = 2$ at the point of maximum (where $k_2x^2 \cong (\alpha + x)\sqrt{2k_5V_1}$). Equations (8) and (9) under the condition $k_2x^2 >> (\alpha l + \beta + x)\sqrt{2k_5V_1}$ (descending branch of a peaked curve) can be transformed into Eqs. (15) and (16), respectively, which express the simple, inversely proportional dependences of reaction rates on x and provide tentative estimates of α and β:

$$V_3 = V_1\alpha l/\varphi x, \quad (15)$$

$$V_{3a} = V_1\beta/\varphi x, \quad (16)$$

where $\varphi = 2$ at the point of maximum (where $k_2x^2 \cong (\alpha l + \beta + x)\sqrt{2k_5V_1}$) and $\varphi = 1$ for the descending branch of the curve. Equation (3) for $V_{3,4}$ under condition (b) transforms into Eq. (15).

For radiation-chemical processes, the rates V in the kinetic equations should be replaced with radiation-chemical yields G using the necessary unit conversion factors and the relationships $V = GP$ and $V_1 = \varepsilon_1 G(R_1^{\bullet})P$, where P is the dose rate, ε_1 is the electron fraction of the saturated component R_1A in the reaction system[100], and $G(R_1^{\bullet})$ is the initial yield of the chain-carrier free radicals (addends) – initiation yield[39,94].

The optimum concentration of the unsaturated component in the system maximizing the process rate, x_m, can be calculated using rate equations (3a), (4a), (8a), and (9a) or the corresponding analytical expressions for k_2 provided that the other parameters involved in these equations are known. This opens up the way to intensification of some technological processes that are based on the addition of free radicals to C=C, C=O, and O=O bonds and occur *via* a nonbranched-chain mechanism through the formation of a 1:1 adduct.

CONCLUSIONS

The above data concerning the competition kinetics of the nonbranched-chain addition of saturated free radicals to the multiple bonds of olefins (and its derivatives), formaldehyde, and oxygen molecules make it possible to describe, using rate equations (1)–(9a), obtained by quasi-steady-state treatment, the peaking experimental dependences of the formation rates of molecular 1:1 adducts on the concentration of the unsaturated compound over the entire range of its variation in binary systems consisting of saturated and unsaturated components (Figs. 1–3). The proposed addition mechanism involves the reaction of a free 1:1 adduct radical with an unsaturated molecule yielding a low-reactive free radical (the reaction 4 competing with the chain propagation reactions in *Schemes 1–4*). In such reaction systems, the unsaturated compound is both a reactant and an autoinhibitor, specifically, a source of low-reactive free radicals shortening kinetic chains. The progressive inhibition of the nonbranched-chain processes, which takes place as the concentration of the unsaturated compound is raised (after the maximum process rate is reached), can be an element of the self-regulation of the natural processes that returns them to the stable steady state.

A similar description is applicable to the nonbranched-chain free-radical hydrogen oxidation in water at 296 K [63] (Fig. 3, curve *2*). Using the hydrogen oxidation mechanism considered here, it has been demonstrated that, in the Earth's upper atmosphere, the decomposition of O_3 in its reaction with the $HO^{\bullet}$ radical can occur *via* the addition of the latter to the ozone molecule, yielding the $HO_4^{\bullet}$ radical, which is capable of efficiently absorbing UV radiation.

REFERENCES

1. Gurvich LV, Karachevtsev GV, Kondrat'ev VN, Lebedev YuA, Medvedev VA, Potapov VK, and Khodeev YuS, Energii razryva khimicheskikh svyazei. Potentsialy ionizatsiii srodstvo k elektronu(Bond Dissociation Energies, Ionization Potentials, and Electron Affinity), Kondrat'ev VN, Editor, Nauka, Moscow, 1974.
2. Benson SW, Thermochemical Kinetics: Methods for the Estimation of Thermochemical Data and Rate Parameters, 2nd Edition, Wiley, New York, 1976.
3. Pedley JB, Naylor RD, and Kirby SP, "Thermochemical Data of Organic Compounds, 2nd Edition, Chapman & Hall, London, 1986.
4. Orlov YuD, Lebedev YuA, and Saifullin ISh, Termokhimiya organicheskikh svobodnykh radikalov (Thermochemistry of Organic Free Radicals), Kutepov AM, Editor., Nauka, Moscow, 2001.
5. Walling Ch, Free Radicals in Solution, Wiley, New

[15]The stabilization energy of the low-reactive free radicals $CH_2=C(CH_3)\dot{C}H_2$, $CH_2=CH\dot{C}HOH$, and $H\dot{C}=O$ in the standard state in the gas phase is –52.0, –42.1, and –24.3 kJ mol^{-1}, respectively[4,99].

York, 1956.
6. Emanuel NM, Denisov ET, and Maizus ZK, Tsepnye reaktsii okisleniya uglevodorodov v zhidkoi faze (Chain Oxidation Reactions of Hydrocarbons in the Liquid Phase), Nauka, Moscow, 1965.
7. Poluektov VA, Babkina EI, and Begishev IR, On the Dependence of the Rate of a Chain Reaction on the Reactant Ratio, Dokady Akademii Nauk SSSR, 1974; 215(3): 649–652.
8. Silaev MM and Bugaenko LT, Mathematical Simulation of the Kinetics of Radiation Induced Hydroxyalkylation of Aliphatic Saturated Alcohols, Radiation Physics and Chemistry, 1992; 40(1): 1–10.
9. Silaev MM and Bugaenko LT, Kinetics of the Addition of α-Hydroxyalkyl Radicals to 2-Propen-1-ol and Formaldehyde, Kinetics and Katalysis, 1994; 35(4): 509–513.
10. Silaev MM, Competition Kinetics of Nonbranched Chain Processes of Free-Radical Addition to Double Bonds of Molecules with the Formation of 1:1 Adducts, Kinetica i Kataliz., 1999; 40(2): 281–284, English Translation in: Kinetics and Catalysis, 1999; 40(2): 256–259.
11. Silaev MM, Simulation of the Nonbranched-Chain Addition of Saturated Free Radicals to Alkenes and Their Derivatives Yielding 1:1 Adducts, Teoreticheskie Osnovy Khimicheskoi Tekhnologii, 2007; 41(3): 280–295, English Translation in: Theoretical Foundations of Chemical Engineering, 2007; 41(3): 273–278.
12. Silaev MM, Simulation of Nonbranched Chain Processes for Producing 1,2-Alkanediols in Alcohol–Formaldehyde Systems, Teoreticheskie Osnovy Khimicheskoi Tekhnologii, 2007; 41(4): 379–384, English Translation in: Thoretical Foundations Chemical Engineering, 2007; 41(4): 357–361.
13. Silaev MM, A New Competitive Kinetic Model of Radical Chain Oxidation: Oxygen as an Autoinhibitor, Biofizika, 2001; 46(2): 203–209, English Translation in: Biophysics, 2001; 46(2): 202–207.
14. Silaev M.M., Simulation of the Initiated Addition of Hydrocarbon Free Radicals and Hydrogen Atoms to Oxygen via a Nonbranched Chain Mechanism, Teoreticheskie Osnovy Khimicheskoi Tekhnologii, 2007; 41(6): 634–642, English Translation in: Theoretical Foundation of Chemical Engineering, 2007; 41(6): 831–838.
15. Bard Y, Nonlinear Parameter Estimation, Academic, New York, 1974.
16. Bateman L, Olefin Oxidation, Quarterly Reviews, 1954; 8(2): 147–167.
17. Urry WH, Stacey FW, Huyser ES, and Juveland OO, The Peroxide- and Light-Induced Additions of Alcohols to Olefins, Journal of the American Chemical Society, 1954; 76(2): 450–455.
18. Urry WH and Juveland OO, Free Radical Additions of Amines to Olefins, Journal of the American Chemical Society, 1958; 80(13): 3322–3328.
19. Shostenko AG, Zagorets PA, Dodonov AM, and Greish AA, γ-Radiation-Induced Addition of Phosphorus Trichloride to Isobutylene, Khimiya Vysokikh Energii, 1970; 4(4): 357.
20. Kim V, Shostenko AG, and Gasparyan MD, Reactivity of Polychloroalkyl Radicals in the Telomerization of CCl_4 with 1-Propene and 2-Methyl-1-Propene (in Russian), Reaction Kinetics and Catalysis Letters, 1979; 12(4): 479–484.
21. Myshkin VE, Shostenko AG, Zagorets PA, Markova KG, and Pchelkin AI, Determination of Absolute Rate Constants for the Addition of the Ethyl Radical to Olefins, Teoreticheskaya i Eksperimental'naya Khimiya, 1977; 13(2): 266–271.
22. Zamyslov RA, Shostenko AG, Dobrov IV, and Tarasova NP, Kinetics of γ-Radiation-Induced Reactions of 2-Propanol with Trifluoropropene and Hexaflu-oropropene, Kinetika I Katalyz., 1987; 28(4): 977–979.
23. Silaev MM, Dependence of Radiation-chemical γ-Diol Yields on the 2-Propen-1-ol Concentration in the Radiolysis of Aliphatic Saturated C_1-C_3 Alcohol + 2-Propen-1-ol Systems, Khimiya Vysokikh Energii, 1990; 24(3): 282–283.
24. Silaev MM, γ-Diol Formation via the Autooxidation of 2-Propen-1-ol Solutions in Saturated Alcohols, Vestnik Moskovskogo Universiteta, Ser. 2: Khimiya, 1994; 35(1): 40–42.
25. Bugaenko LT, Kuzmin MG, and Polak LS, High-Energy Chemistry, Horwood Hall, New York, 1993, p. 112.
26. Thomas JK, Pulse Radiolysis of Aqueous Solutions of Methyl Iodide and Methyl Bromide. The Reactions of Iodine Atoms and Methyl Radicals in Water The Journal of the Physical Chemistry, 1967; 71(6): 1919–1925.
27. Ogorodnikov SK, Formal'degid (Formaldehyde), Khimiya, Leningrad, 1984.
28. Silaev MM, Rudnev AV, and Kalyazin EP, Formaldehyde. III. Concentration of Free Formaldehyde as a Function of Temperature, Polarity of Solvents, and Total Concentration of Formaldehyde in Solution, Zhurnal Fizicheskoi Khimii, 1979; 53(7): 1647–1651.
29. Oyama M., A Free-Radical Reaction of Primary and Secondary Alcohols with Formaldehyde, the Journal of Organic Chemistry, 1965; 30(7): 2429–2432.
30. Nikitin GI, Lefor D, and Vorob'ev ED, Free Radical Reaction of Primary Alcohols with Formaldehyde, Izvestiya Akademii Nauk SSSR, Ser. Khimiya, 1966(7): 1271–1272.
31. Dzhurinskaya MB, Rudnev AV, and Kalyazin EP, High Temperature UV Photolysis of Formaldehyde in Liquid Methanol, Vestnik Moskovskogo Universiteta, Ser. 2: Khimiya, 1984; 25(2): 173–176.
32. Kalyazin EP, Petryaev EP, and Shadyro OI, Reaction between Oxyalkyl Radicals and Aldehydes, Zhurnal Organicheskoi Khimii, 1977; 13(2): 293–295.
33. Novoselov AI, Silaev MM, and Bugaenko LT, Effect

of Temperature on the Yields of Final Products in the γ-Radiolysis of Formaldehyde Solutions in C_1-C_3 Alkanols, Khimiya Vysokich Energii, 2004; 38(4): 270–272, English Translation in: High Energy Chemistry, 2004; 38(4): 236–238.
34. Novoselov AI, M. Silaev MM, and Bugaenko LT, Dependence of Ethanediol Yield on Formaldehyde Concentration in γ-Radiolysis of Methanol–Formaldehyde System at 373–473 K, Khimiya Vysokikh Energii, 2008; 42(1): 74–75, English Translation in: High Energy Chemistry, 2008; 42(1): 69–70.
35. Novoselov AI, Silaev MM, and Bugaenko LT, γ-Induced Single-Step Synthesis of Ethylene Glycol from Methanol–Formaldehyde Solution, Theoreticheskie Osnovy Khimicheskoy Tekhnologii, 2010; 44(4): 450–453, English Translation in: Theoretical Foundation of Chemical Engineering, 2010; 44(4): 432–435.
36. Novoselov AI, Silaev MM, and Bugaenko LT, Dependence of 1,2-Propanediol Yield on Formaldehyde Concentration in γ-Radiolysis of Ethanol–Formaldehyde System at 373473 K, Khimiya Vysokikh Energii, 2007; 41(1): 58, English Translation in: High Energy Chemistry, 2207; 41(1): 53.
37. Pshezhetskii SYa, Kotov AG, Milinchuk VK, Roginskii VA, and Tupikov VI, EPR svobodnykh radikalov v radiatsionnoi khimii" ("ESR of Free Radicals in Radiation Chemistry"), Khimiya, Moscow, 1972.
38. Silaev MM, Estimating the Solvent Concentration in Formaldehyde Solutions at Various Temperatures, Zhurnal Fizicheskoy Khimii, 1993; 67(9): 1944.
39. Silaev MM, Applied Aspects of the γ-Radiolysis of C_1-C_4 Alcohols and Binary Mixtures on Their Basis, Khimiya Vysokikh Energii, 2002; 36(2): 97–101, English Translation in: High Energy Chemistry, 2002; 36(2): 70–74.
40. Silaev MM, Bugaenko LT, and Kalyazin EP, On the Possibility of Adequately Estimating the Rate Constants for the Reaction of Hydroxyalkyl Radicals with Each Other Using the Self-Diffusion Coefficients or Viscosities of the Corresponding Alcohols, Vestnik Moskovskogo. Univiversiteta, Ser. 2: Khimiya, 1986; 27(4): 386–389.
41. Shadyro OI, Radiation-chemical Conversions of Aldehydes in Various Systems, Ph.D. Thesis (Chemistry), Belarusian State University, Minsk, 1975.
42. Silaev MM, Relative Reactivity of α-Hydroxyethyl Radicals for 2-Propene-1-ol and Formaldehyde Double-Bond Addition, Vestnik Moskovskogo Universiteta, Ser. 2: Khimiya, 1993; 34(3): 311.
43. Seki H, Nagai R, and Imamura M, γ-Radiolysis of a Binary Mixture of Methanol and Water. The Formation of Formaldehyde in the Radiolysis of Liquid Methanol, Bulletin of the Chemical Society of Japan., 1968; 41(12): 2877–2881.
44. Shtern VYa, Mekhanizm okisleniya uglevodorodov v gazovoi faze (Mechanism of the Gas-Phase Oxidation of Hydrocarbons), Akademiya Nauk SSSR, Moscow, 1960.
45. Bäckström HLJ, Der Kettenmechanismus bei der Autoxydation von Aldehyden, Zeitschrift für physikalische Chemie (B), 1934; 25(1–2): 99–121.
46. Aliev AA, and Saraeva VV, Isomerization of Peroxy Radicals Resulting from the Radiation-Induced Oxidation of o-Xylene, Vestnik Moskovskogo Universiteta, Ser. 2: Khimiya, 1983; 34(4): 371–374.
47. Badin EJ, The Reaction between Atomic Hydrogen and Molecular Oxygen at Low Pressures. Surface Effects, Journal of the American Chemistry Society, 1948; 70(11): 3651–3655.
48. Buchachenko AL, Kompleksy radikalov i molekulyarnogo kisloroda s organicheskimi molekulami (Complexes of Radicals and Dioxygen with Organic Molecules), Beletskaya IP, Editor, Nauka, Moscow, 1984.
49. Francisco JS and Williams IH, "The Thermochemistry of Polyoxides and Polyoxy Radicals, International Journal of Chemical Kinetics, 1988; 20(6): 455–466.
50. Kokorev VN, Vyshinskii NN, Maslennikov VP, Abronin IA, Zhidomirov GM, and Aleksandrov YuA, Electronic Structure and Chemical Reactions of Peroxides: I. MINDO/3 Calculation of the Geometry and Enthalpy of Formation of the Ground States of Organic and Organoelement Peroxides", Zhurnal Strukturnoi Khimii, 1981; 22(4): 9–15.
51. Dmitruk AF, Lobanov VV, and Kholoimova LI, Role of Tetroxide Conformation in the Mechanism of Peroxy Radical Recombination, Teoreticheskaya I Eksperimental'naya Khimiya, 1986; 22(3): 363–366.
52. Belyakov VA, Vasil'ev RF, Ivanova NM, Minaev BF, Osyaeva OV, and Fedorova GF, Electronic Model of the Excitation of Chemiluminescence in the Oxidation of Organic Compounds, Izvestiya Akademii Nauk SSSR, Ser.: Fizika, 1987; 51(3): 540–547.
53. Ase P, Bock W, and Snelson A, Alkylperoxy and Alkyl Radicals. 1. Infrared Spectra of CH_3O_2 and $CH_3O_4CH_3$ and the Ultraviolet Photolysis of CH_3O_2 in Argon + Oxygen Matrices, the Journal of Physical Chemistry, 1986; 90(10): 2099–2109.
54. Pimentel GC and McClellan AL, the Hydrogen Bond, Pauling L, Editor, Freeman, San Francisco, 1960, p. 200.
55. Russell GA, Deuterium-Isotope Effects in the Autooxidation of Aralkyl Hydrocarbons: Mechanism of the Interaction of Peroxy Radicals, Journal of the American Chemical Society, 1957; 79(14): 3871–3877.
56. Silaev MM, The Competition Kinetics of Nonbranched Chain Processes of Free-Radical Addition to Double Bonds of Molecules with the Formation of 1:1 Adducts and the Inhibition by the Substrate, Oxidation Communication, 1999; 22(2):

159–170.
57. Silaev MM, The Competition Kinetics of Radical-Chain Addition, Zhurnal Fizicheskoi Khimii, 1999; 73(7): 1180–1184, English Translation in: Russian Journal of Physical Chemistry, 1999; 73(7): 1050–1054.
58. Darmanyan AP, Gregory DD, Guo Y, Jenks WS, Burel L, Eloy D, and Jardon P, Quenching of Singlet Oxygen by Oxygen- and Sulfur-Centered Radicals: Evidence for Energy Transfer to Peroxy Radicals in Solution, Journal of the American Chemistry Society, 1998; 120(2); 396–403.
59. Kanofsky JR, Singlet Oxygen Production from the Reactions of Alkylperoxy Radicals. Evidence from 1268-nm Chemiluminescence, The Journal of Organic Chemistry, 1986; 51(17): 3386–3388.
60. Semenov NN, Tsepnye reaktsii (Chain Reactions), Goskhimtekhizdat, Leningrad, 1934, pp. 241, 203.
61. Reznikovskii M, Tarasova Z, and Dogadkin B, Oxygen Solubility in Some Organic Liquids, Zhurnal Obshchei Khimii, 1950; 20(1): 63–67.
62. Howard JA and Ingold KU, Absolute Rate Constants for Hydrocarbon Autooxidation. VI. Alkyl Aromatic and Olefinic Hydrocarbons, Canadian Journal of Chemistry, 1967; 45(8): 793–802.
63. Barr NF and Allen AO, Hydrogen Atoms in the Radiolysis of Water, the Journal of Physical Chemistry, 1959; 63(6): 928–931.
64. Smith HA and Napravnik A, Photochemical Oxidation of Hydrogen, Journal of the American Chemistry Society, 1940; 62(1): 385–393.
65. Pagsberg PB, Eriksen J, and Christensen HC, Pulse Radiolysis of Gaseous Ammonia–Oxygen Mixtures, The Journal of Physical Chemistry, 1979; 83(5): 582–590.
66. Silaev MM, Competitive Mechanism of the Non-branched Radical Chain Oxidation of Hydrogen Involving the Free Cyclohydrotetraoxyl Radical $[\dot{O}O\cdots H\cdots O\dot{O}]^{\bullet}$, Which Inhibits the Chain Process, "Khimiya Vysokikh Energii, 2003; 37(1): 27–32, English Translation in: High Energy Chemistry, 2003; 37(1): 24–28.
67. Silaev MM, Simulation of Initiated Nonbranched Chain Oxidation of Hydrogen: Oxygen as an Autoinhibitor, Khimiya Vysokich Energii, 2008; 42(2): 124–129, English Translation in: High Energy Chemistry, 2008; 42(1): 95–100.
68. McKay DJ and Wright JS, How Long Can You Make an Oxygen Chain?, Journal of the American Chemistry Society, 1998; 120(5): 1003–1013.
69. Lipikhin NP, Dimers, Clusters, and Cluster Ions of Oxygen in the Gas Phase, Uspekhi Khimii, 1975; 44(8): 366–376.
70. Razumovskii SD, Kislorod – elementarnye formy i svoistva ("Oxygen: Elementary Forms and Properties"), Khimiya, Moscow, 1979.
71. Dunn KM, Scuceria GE, and Schaefer III HF, The infrared spectrum of cyclotetraoxygen, O_4: a theoretical investigation employing the single and double excitation coupled cluster method, The Journal of Chemical Physics, 1990; 92(10): 6077–6080.
72. Brown L and Vaida V, Photoreactivity of Oxygen Dimers in the Ultraviolet, the Journal of Physical Chemistry, 1996; 100(19): 7849–7853.
73. Aquilanti V, Ascenzi D, Bartolomei M, Cappelletti D, Cavalli S, de Castro-Vitores M, and Pirani F, Molecular Beam Scattering of Aligned Oxygen Molecules. The Nature of the Bond in the O_2–O_2 Dimer, Journal of the American Chemistry Society, 1999; 121(46): 10794–1080.
74. Cacace F, de Petris G, and Troiani A, Experimental Detection of Tetraoxygen, Angewandte Chemie, Internation Edition (in English), 2001; 40(21): 4062–4065.
75. Taylor HS, Photosensitisation and the Mechanism of Chemical Reactions, Transactions of the Faraday Society, 1926; 21(63/3): 560–568.
76. Nalbandyan AB and Voevodskii VV, Mekhanizm okisleniya i goreniya vodoroda (Mechanism of Hydrogen Oxidation and Combustion), Kondrat'ev VN, Editor, Akad. Nauk SSSR, Moscow, 1949.
77. Foner SN and Hudson RL, Mass spectrometry of the HO_2 free radical, The Journal of Chemical Physics, 1962; 36(10): 2681.
78. Hochanadel CJ, Ghormley JA, and Ogren PJ, Absorption Spectrum and Reaction Kinetics of the HO_2 Radical in the Gas Phase, the Journal of Chemical Physics, 1972; 56(9): 4426–4432.
79. Robertson JB, A Mass Spectral Search for H_2O_4 and HO_4 in a Gaseous Mixture Containing HO_2 and O_2, Chemistry and Industry, 1954; 48: 1485.
80. Bahnemann D and Hart EJ, Rate Constants of the Reaction of the Hydrated Electron and Hydroxyl Radical with Ozone in Aqueous Solution, the Journal of Physical Chemistry, 1982; 86(2): 252–255.
81. Vodorodnaya svyaz: Sbornik statei (The Hydrogen Bonding: Collection of Articles) Sokolov ND, Editor, Nauka, Moscow, 1981.
82. Staehelin J, Bühler RE, and Hoigné J, Ozone Decomposition in Water Studied by Pulse Radiolysis. 2. OH and HO_4 as Chain Intermediates, the Journal of Physical Chemistry, 1984; 88(24): 5999–6004.
83. Cacace F, de Petris G, Pepi F, and Troiani A, Experimental Detection of Hydrogen Trioxide, Science, 1999; 285(5424): 81–82.
84. Bühler RF, Staehelin J, and Hoigné J, Ozone Decomposition in Water Studied by Pulse Radiolysis. 1. HO_2/O_2^- and HO_3/O_3^- as Intermediates", The Journal of Physical Chemistry, 1984; 88(12): 2560–2564.
85. Trushkov IV, Silaev MM, and Chuvylkin ND, Acyclic and Cyclic Forms of the Radicals $HO_4^{\bullet}$, $CH_3O_4^{\bullet}$, and $C_2H_5O_4^{\bullet}$: Ab Initio Quantum Chemical Calculations, Izvestiya Akademii Nauk, Ser.: Khimiya, No. 3, 2009, pp. 479–482, English Translation in: Russian Chemical Bulletin,

International Edition, 2009; 58(3): 489–492.
86. Mansergas A, Anglada JM, Olivella S, Ruiz-López MF, "On the Nature of the Unusually Long OO Bond in HO_3 and HO_4 Radicals", Phys. Chem. Chem. Phys., 2007; 9(44): 5865–5873.
87. Wong W and Davis DD, A Flash Photolysis Resonance Fluorescence Study of the Reactions of Atomic Hydrogen and Molecular Oxygen: $H + O_2 + M \rightarrow HO_2 + M$, International Journal of Chemical Kinetics, 1974; 6(3): 401–416.
88. Xu X, Muller RP, and Goddard III WA, The Gas Phase Reaction of Singlet Dioxygen with Water: a Water-Catalyzed Mechanism, Proceedings of the National Academy Sciences of the United States of America, 2002, 99(6): 3376–3381.
89. Seidl ET and Schaefer III HF, Is There a Transition State for the Unimolecular Dissociation of Cyclotetraoxygen (O_4)?, The Journal of Chemical Physics, 1992; 96(2): 1176–1182.
90. Hernández-Lamoneda R and Ramírez-Solís A, Reactivity and Electronic States of O_4 along Minimum Energy Paths, the Journal of Chemical Physics, 2000; 113(10): 4139–4145.
91. Varandas AJC and Zhang L, Test Studies on the Potential Energy Surface and Rate Constant for the $OH + O_3$ Atmospheric Reaction, Chemical Physics Letters, 2000; 331(5–6): 474–482.
92. Atmosfera. Spravochnik (Atmosphere: A Handbook), Gidrometeoizdat, Leningrad, 1991.
93. Okabe H, "Photochemistry of Small Molecules", Wiley, New York, 1978.
94. Pikaev AK, Sovremennaya radiatsionnaya khimiya. Radioliz gazov i zhidkostei ("Modern Radiation Chemistry: Radiolysis of Gases and Liquids"), Nauka, Moscow, 1986.
95. Boyd AW, Willis C, and Miller OA, A Re-examination of the Yields in the High Dose Rate Radiolysis of Gaseous Ammonia, Canadian Journal of Chemistry, 1971; 49(13): 2283–2289.
96. Silaev MM, Competition Mechanism of Substrate-Inhibited Radical Chain Addition to Double Bond, Neftekhimiya, 2000; 40 (1): 33–40, English Translation in: Peroleum Chemistry, 2000; 40(1): 29–35.
97. Silaev MM, Competition Kinetics of Nonbranched Chain Processes of Free Radical Addition to the C=C, C=O, and O=O Double Bonds of Molecules, Neftekhimiya, 2003; 43(4): 302–307, English Translation in: Petroleum Chemistry, 2003; 43(4): 258–273.
98. Silaev MM, Low-reactive Free Radicals Inhibiting Nonbranched Chain Processes of Addition, Biofizika, 2005; 50(4): 585–600, English Translation in: Biophysics, 2005; 50(4): 511–524.
99. Sanderson RT, Radical Reorganization and Bond Energies in Organic Molecules, The Journal of Organic Chemistry, 1982; 47(20): 3835–3839.
100. Vereshchinskii IV and Pikaev AK, Vvedenie V radiatsionnuyu khimiyu (Introduction to Radiation Chemistry), Spitsyn, V.I., Editor, Akademiya Nauk SSSR, Moscow, 1963, p. 190.

Source of support: Nil, Conflict of interest: None Declared